

Low-energy neutrino-nucleus cross sections

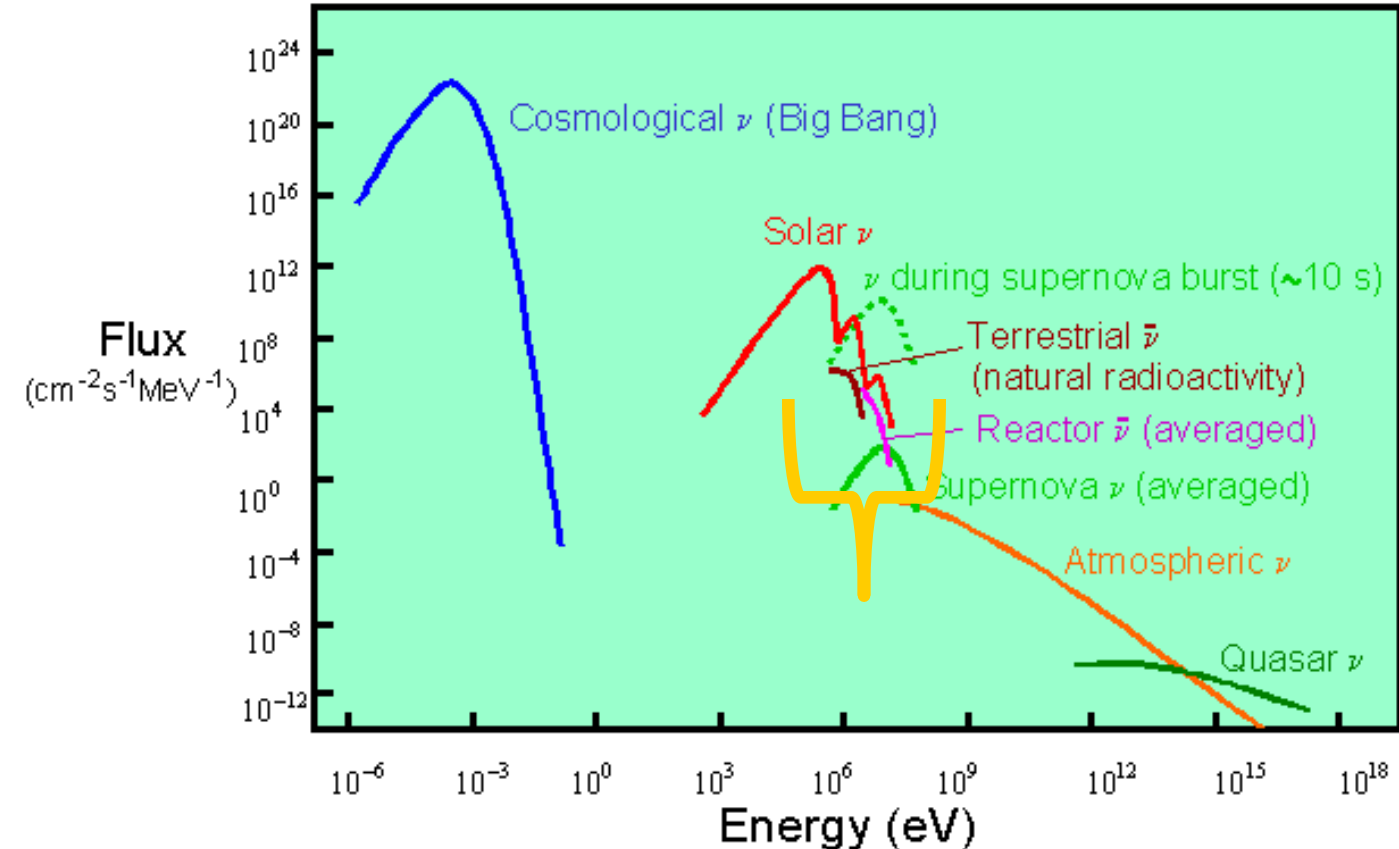
N. Jachowicz

Ghent University
Department of Physics and Astronomy

natalie.jachowicz@UGent.be



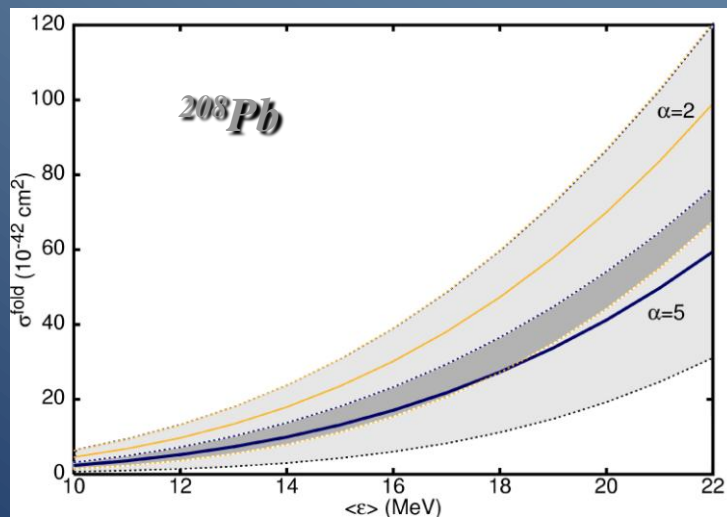
Neutrino energies



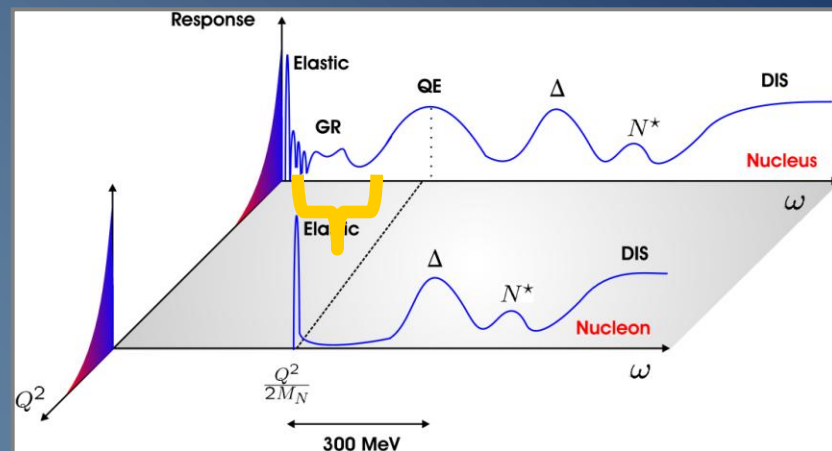
Flux on earth of neutrinos from various sources, in function of energy

Neutrino-hadron scattering ?

- little experimental data is available
 - small cross sections
 - no monochromatic neutrino beams



N.J. et al, PRC66, 065501 (2002) ;
 E. Kolbe et al, PRC63, 025802 (2001) ;
 J. Engel et al, PRD67, 013005 (2001)



Uncertainties :

- one has to rely on theoretical predictions,
- uncertainties induced by model dependence
- and more fundamental uncertainties ...

What can we Learn from these neutrinos ?

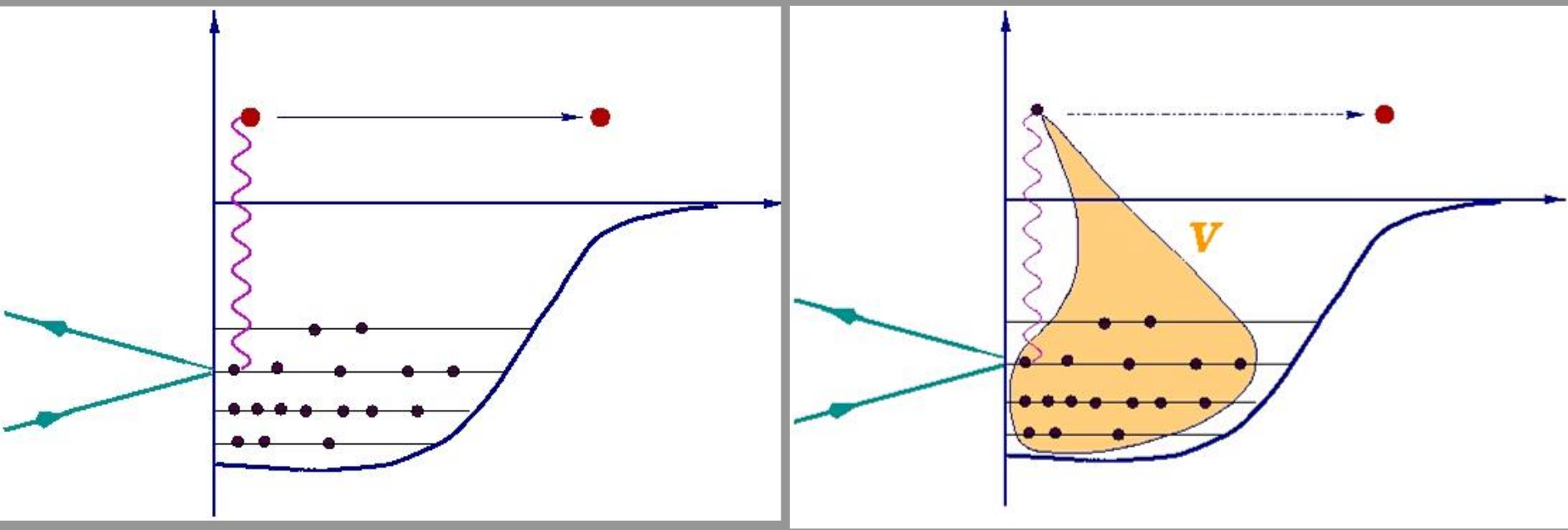
- Electroweak tests
- Nuclear structure information
- Neutrino oscillations
- Astrophysical neutrinos : a.o. core-collapse supernovae
- Neutronucleosynthesis

How can we Learn from these neutrinos ?

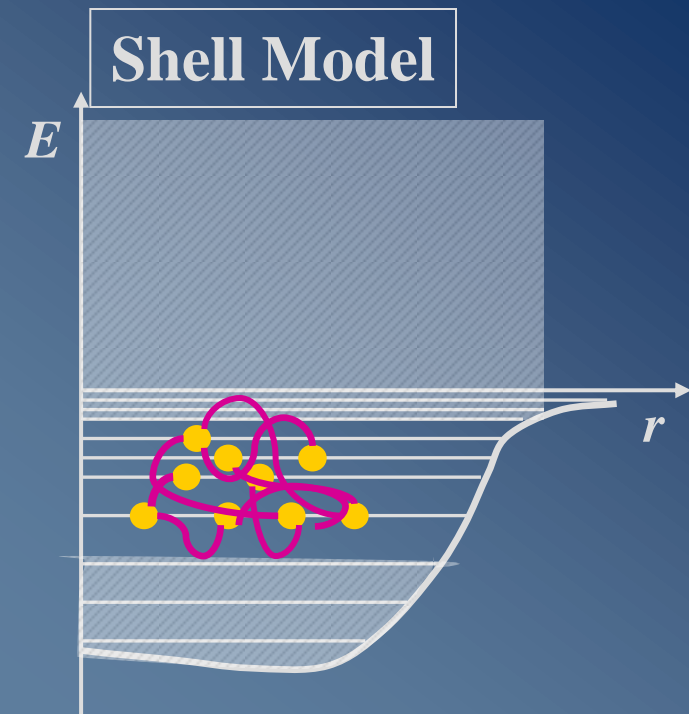
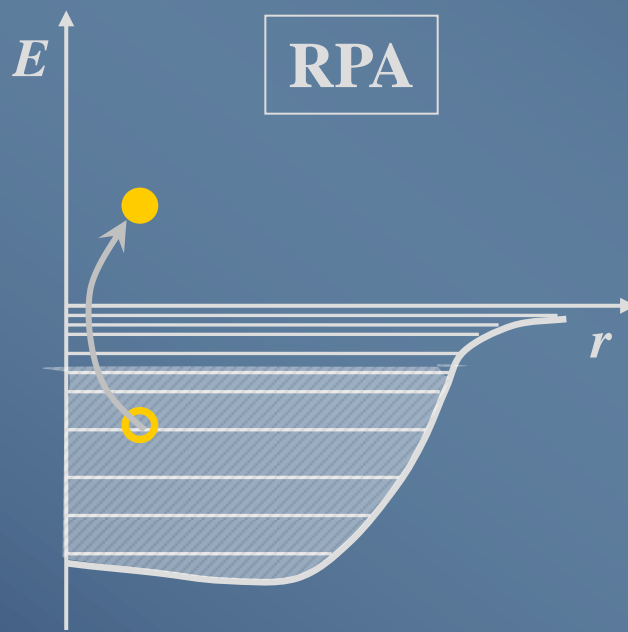
- Detect them
 - Neutrino-electron scattering
 - Neutrino-hadron scattering
- Study their interactions : theory + experiment

Modeling neutrino-nucleus cross sections :

RPA



Modeling neutrino-nucleus cross sections :



E. Kolbe, K. Langanke, S. Krewald, F.K. Thielemann, NPA540, 599 (1992), H. Kim, J. Piekarewicz, C. Horowitz, PRC51, 2739 (1994), S. Singh, N. Mukhopadhyay and E. Oset, PRC57, 2687 (1998), N.J., S. Rombouts, K. Heyde, PRC56, 3246 (1999), A. Hayes, I. Towner, PRC61, 044603 (2000), C. Volpe, N. Auerbach, G. Coló, T. Suzuki, N. Van Giai, PRC62, 015501 (2000), N.J. K. Heyde, J. Ryckebusch, PRC65, 025501(2002), E. Kolbe, K. Langanke, G. Martínez-Pinedo, P. Vogel, J. Phys.G29, 2569 (2003), A. Samana, F. Krmpotić, N. Paar, C. Bertulani, PRC83, 024303 (2011), ...

Low-energy neutrino-nucleus cross sections

Lepton tensor

$$l_{\alpha\beta} \equiv \overline{\sum_{s,s'}} [\bar{u}_l \gamma_\alpha (1 - \gamma_5) u_l]^\dagger [\bar{u}_\nu \gamma_\beta (1 - \gamma_5) u_\nu]$$

Hadronic current

$$J^\mu = F_1(Q^2)\gamma^\mu + i\frac{\kappa}{2M_N}F_2(Q^2)\sigma^{\mu\nu}q_\nu + G_A(Q^2)\gamma^\mu\gamma_5 + \frac{1}{2M_N}G_P(Q^2)q^\mu\gamma_5$$

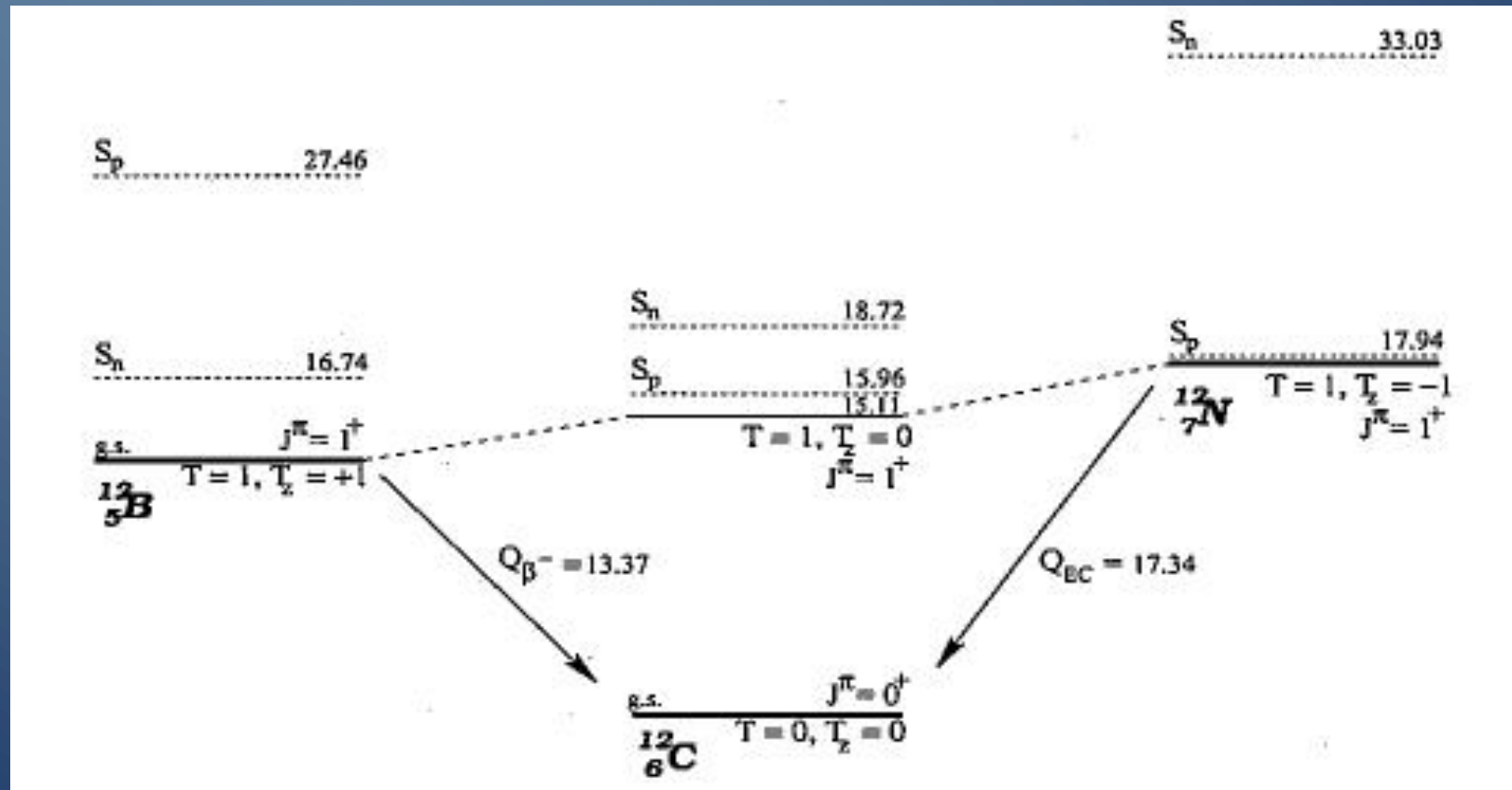
$$\left(\frac{d^2\sigma_{i \rightarrow f}}{d\Omega d\omega} \right)_{\frac{\nu}{\bar{\nu}}} = \frac{G^2 \varepsilon_f^2}{\pi} \frac{2 \cos^2\left(\frac{\theta}{2}\right)}{2J_i + 1} \left[\sum_{J=0}^{\infty} \sigma_{OL}^J + \sum_{J=1}^{\infty} \sigma_T^J \right]$$

$$\sigma_{OL}^J = \left| \left\langle J_f \left| \left| \widehat{\mathcal{M}}_J(\kappa) + \frac{\omega}{|\vec{q}|} \widehat{\mathcal{L}}_J(\kappa) \right| \right| J_i \right\rangle \right|^2$$

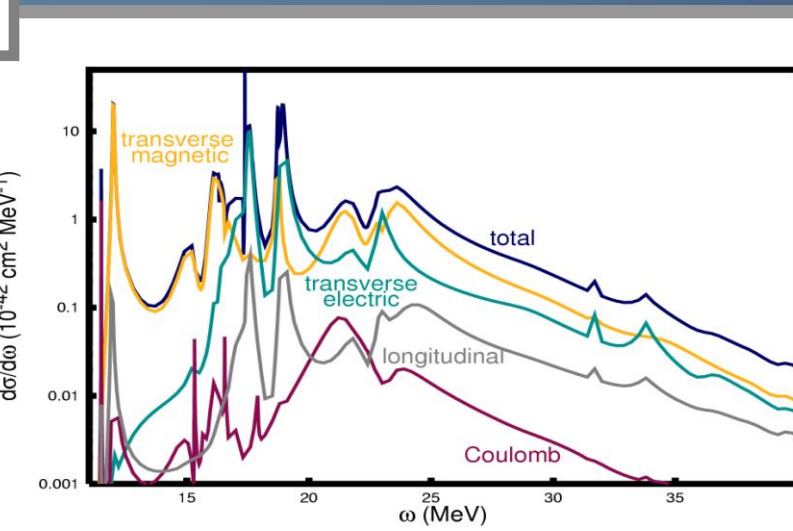
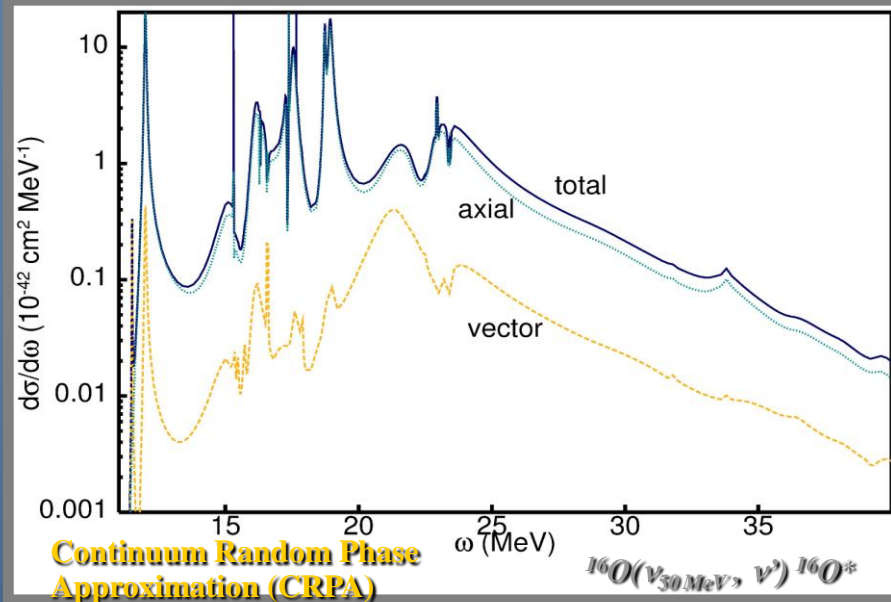
$$\begin{aligned} \sigma_T^J &= \left(-\frac{q_\mu^2}{2|\vec{q}|^2} + \tan^2\left(\frac{\theta}{2}\right) \right) \left[\left| \left\langle J_f \left| \left| \widehat{\mathcal{J}}_J^{mag}(\kappa) \right| \right| J_i \right\rangle \right|^2 + \left| \left\langle J_f \left| \left| \widehat{\mathcal{J}}_J^{el}(\kappa) \right| \right| J_i \right\rangle \right|^2 \right] \\ &\mp \tan\left(\frac{\theta}{2}\right) \sqrt{-\frac{q_\mu^2}{|\vec{q}|^2} + \tan^2\left(\frac{\theta}{2}\right)} \left[2\Re \left(\left\langle J_f \left| \left| \widehat{\mathcal{J}}_J^{mag}(\kappa) \right| \right| J_i \right\rangle \left\langle J_f \left| \left| \widehat{\mathcal{J}}_J^{el}(\kappa) \right| \right| J_i \right\rangle^* \right) \right] \end{aligned}$$

Low-energy neutrino-nucleus cross sections

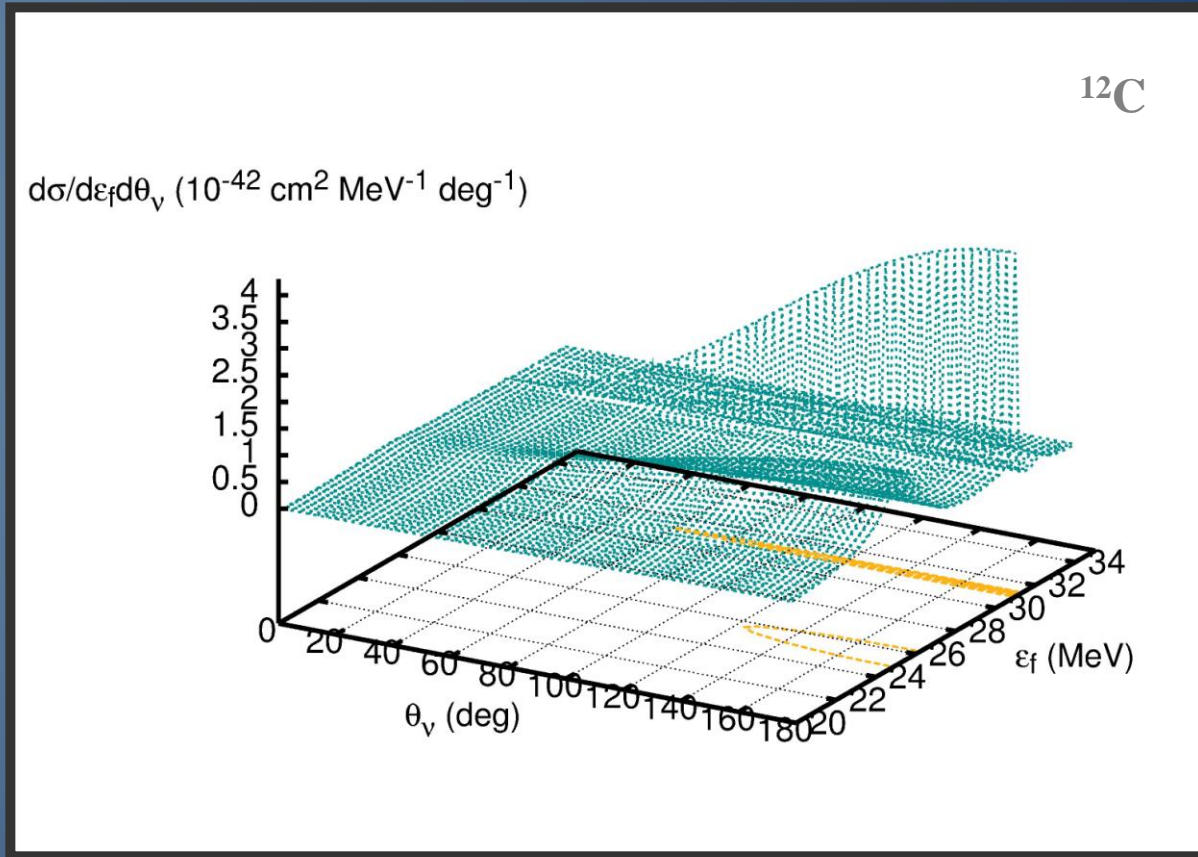
Target nuclei : ^{12}C , ^{16}O , ^{56}Fe , ^{208}Pb



Low-energy neutrino-nucleus cross sections

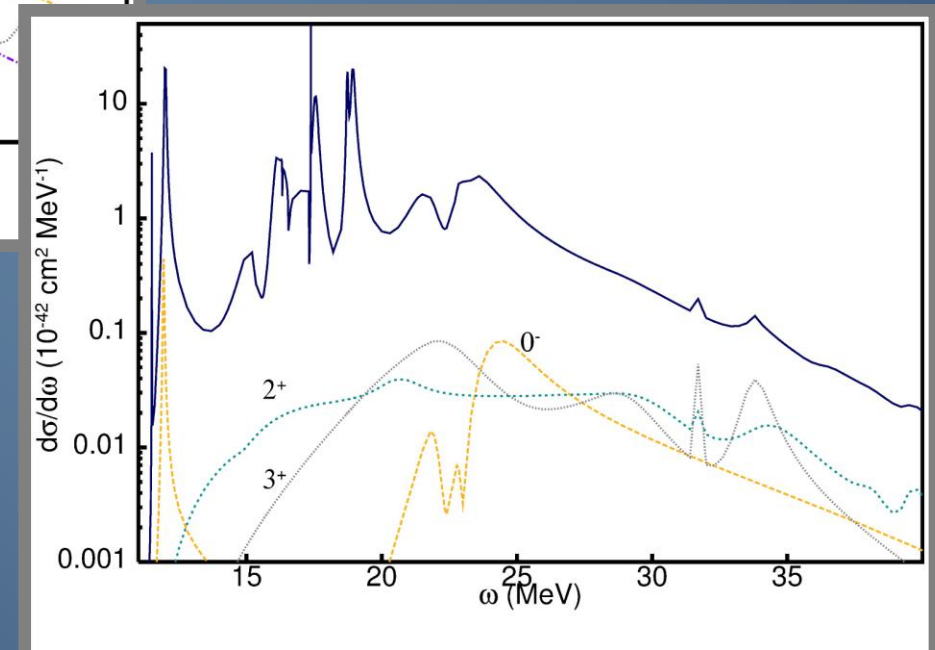
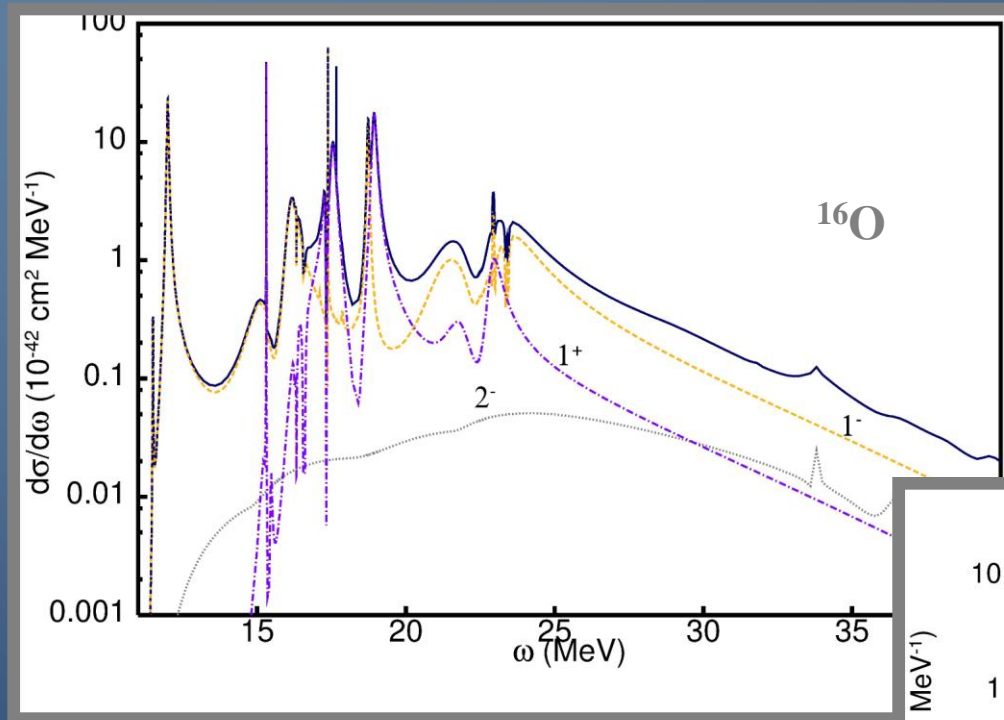


Low-energy neutrino-nucleus cross sections



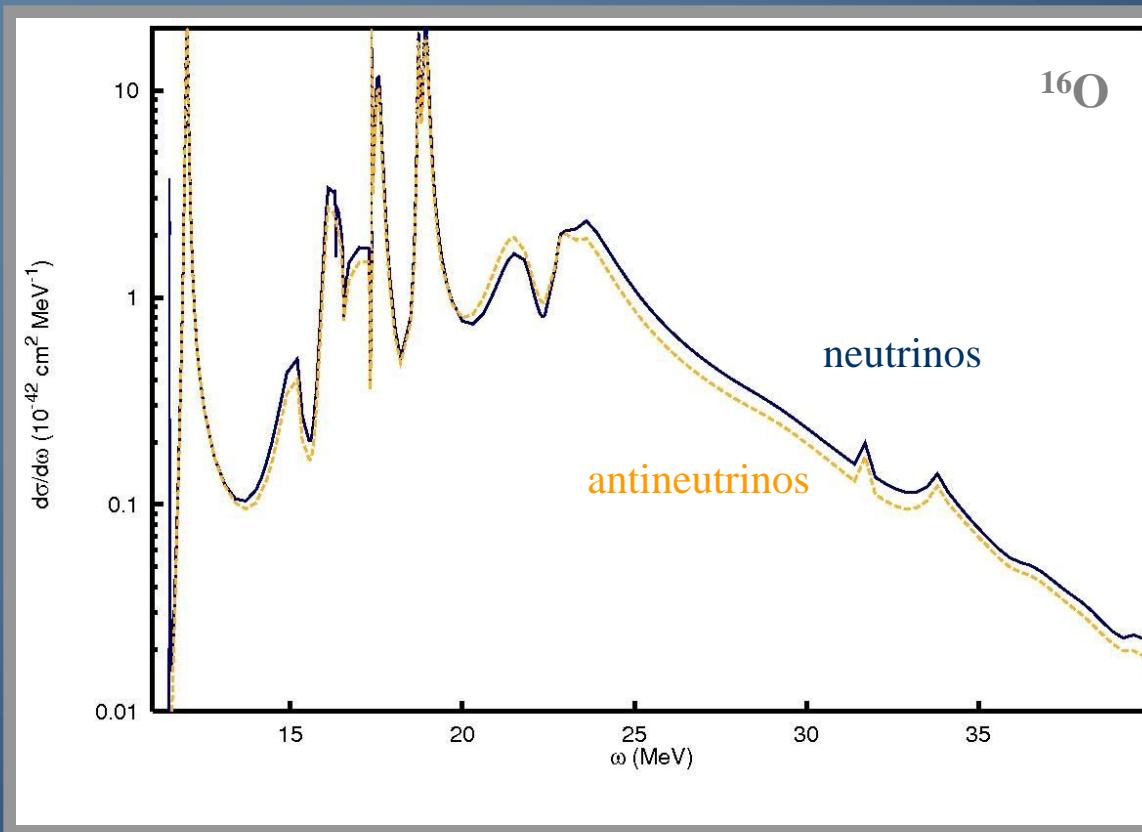
Low-energy neutrino-nucleus cross sections

Higher order multipoles important :

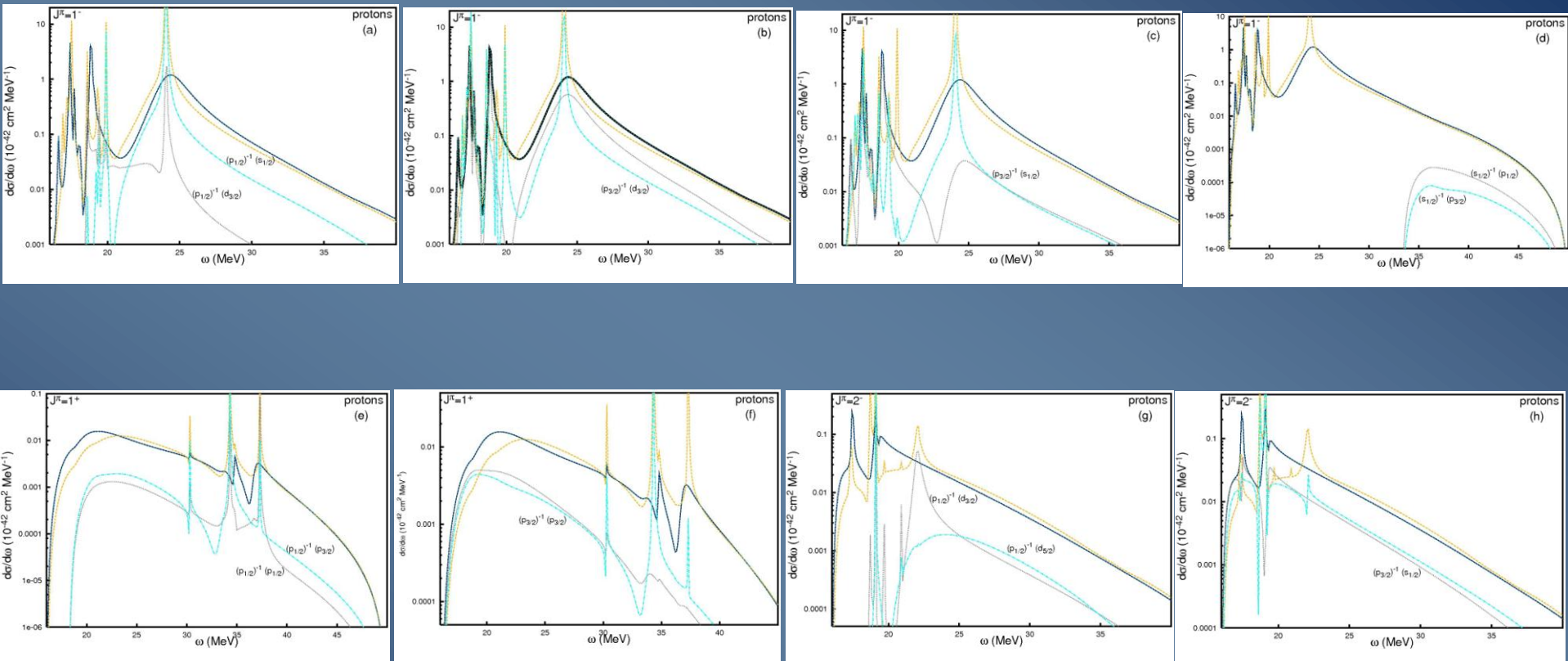


Low-energy neutrino-nucleus cross sections

Neutrinos versus antineutrinos



Contribution of different single-particle channels in ^{12}C

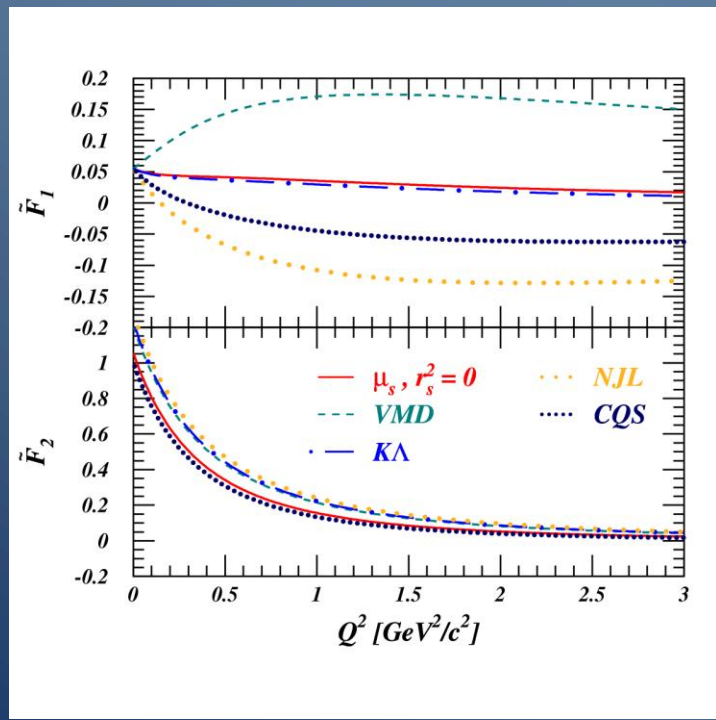


Strangeness in the nucleon

Axial form factor :

$$G_A(Q^2) = -\frac{(\tau_3 g_A - g_A^s)}{2} G(Q^2), \quad g_A = 1.262$$

$$G(Q^2) = (1 + Q^2/M^2)^{-2}, \quad M = 1.032$$



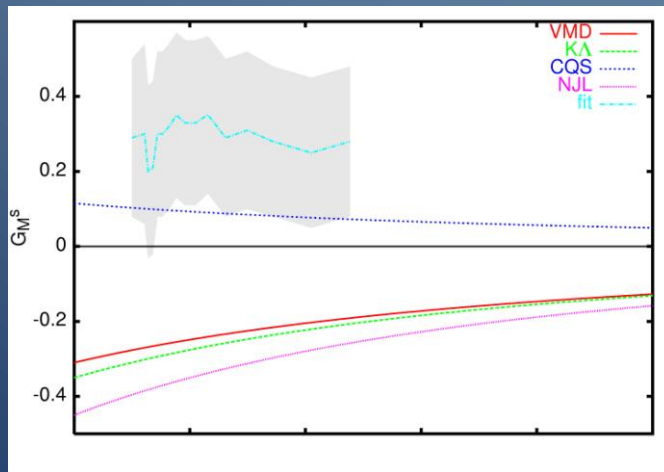
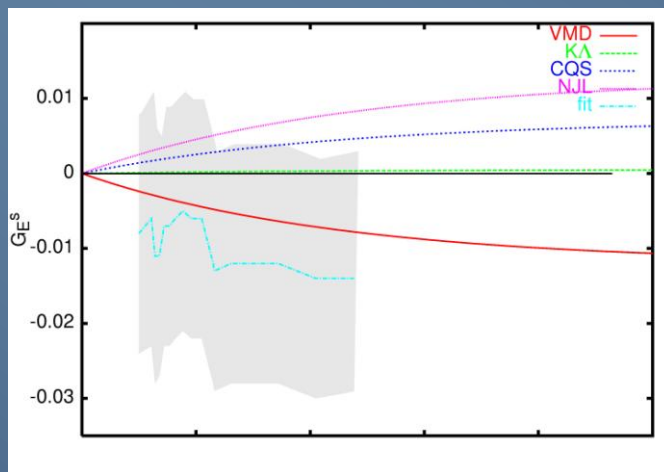
Weak vector form factors :

$$F_1^s = \frac{1}{6} \frac{-r_s^2 Q^2}{(1 + Q^2/M_1^2)^2}, \quad M_1 = 1.3$$

$$F_2^s = \frac{\mu_s}{(1 + Q^2/M_2^2)^2}, \quad M_2 = 1.26$$

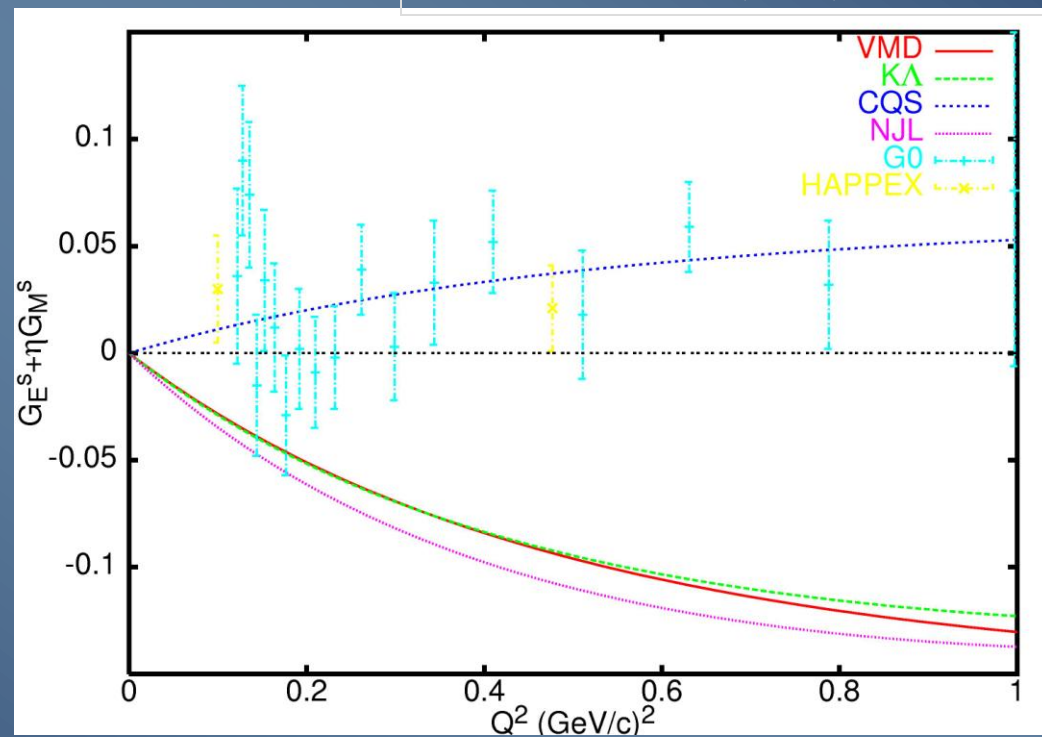
Model	$\mu_s(\mu_N)$	$r_s^2(\text{fm}^2)$
VMD	-0.31	0.16
K Λ	-0.35	-0.007
NJL	-0.45	-0.17
CQS (K)	0.115	-0.095

Low-energy neutrino-nucleus cross sections



Model	$\mu_s(\mu_N)$	$r_s^2(\text{fm}^2)$
VMD	-0.31	0.16
KA	-0.35	-0.007
NJL	-0.45	-0.17
CQS (K)	0.115	-0.095

Data and fit from ‘Global analysis of nucleon strange form factors at low Q^2 ’, J. Liu, R.D. McKeown, R.D. Ramsey-Musolf, PRC76, 025202 (2007).



Low-energy neutrino-nucleus cross sections

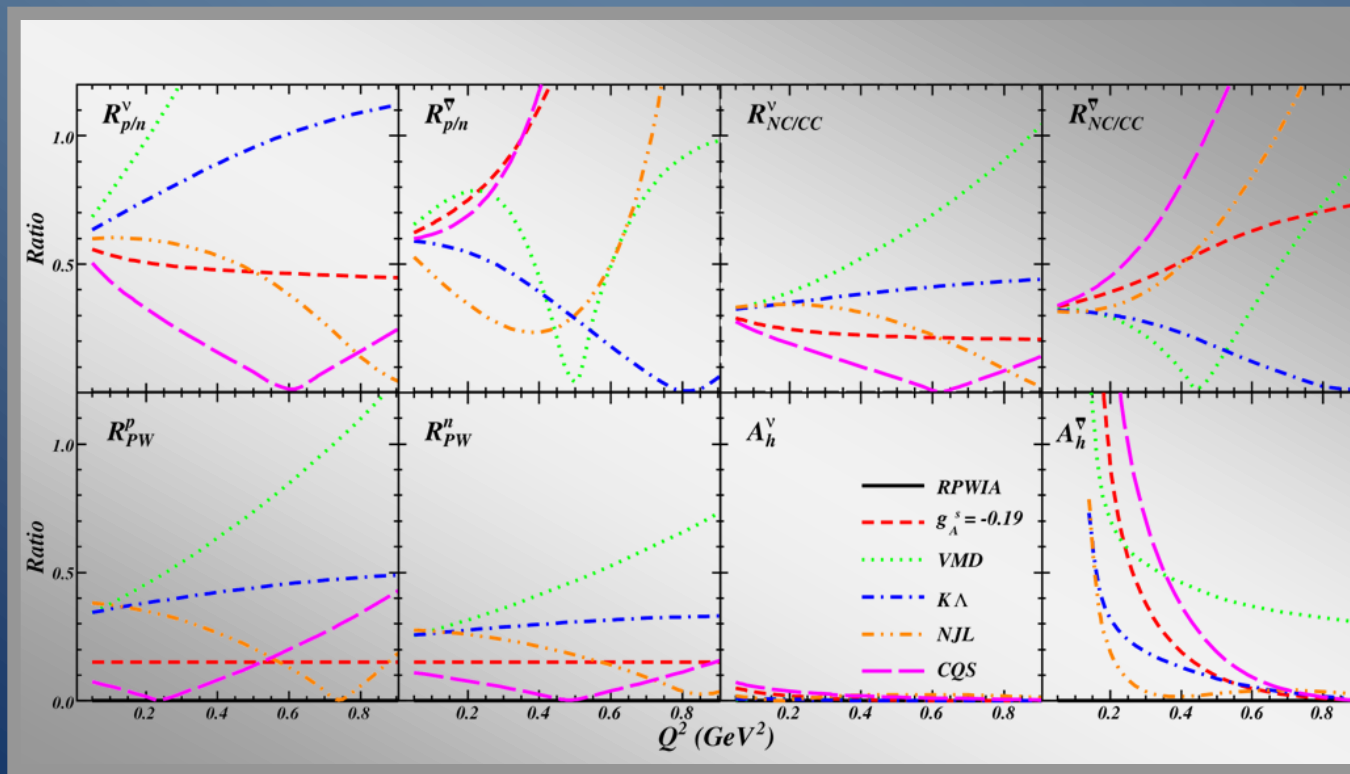
Traditionally :

- strangeness contribution to the ***weak vector formfactors*** : Parity Violating Electron Scattering
(Sample, Happex, G0, ...)



- strangeness contribution to the ***axial current*** : neutrino scattering

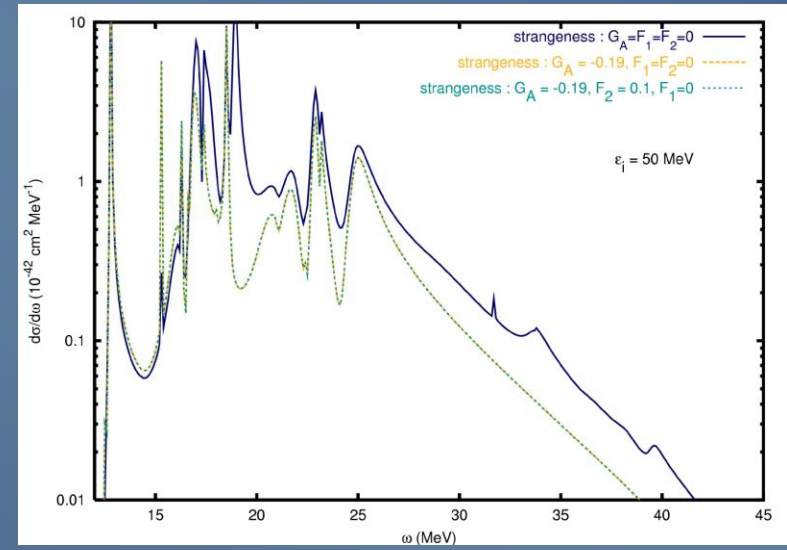
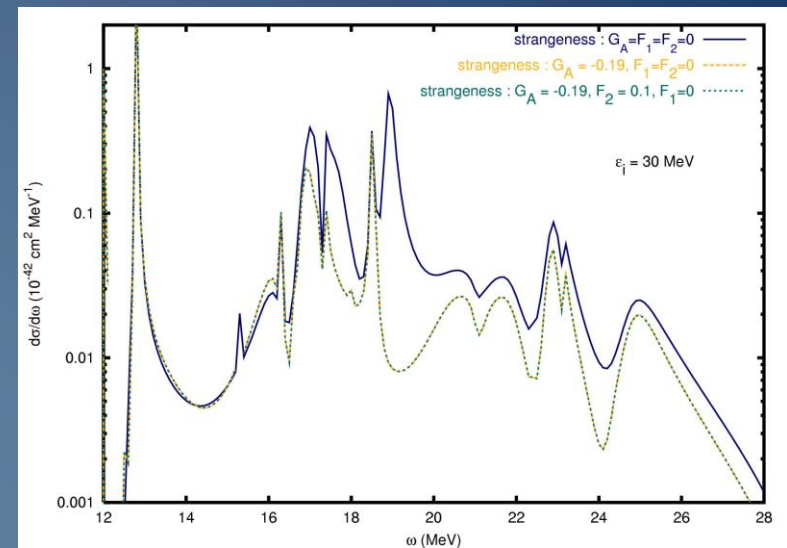
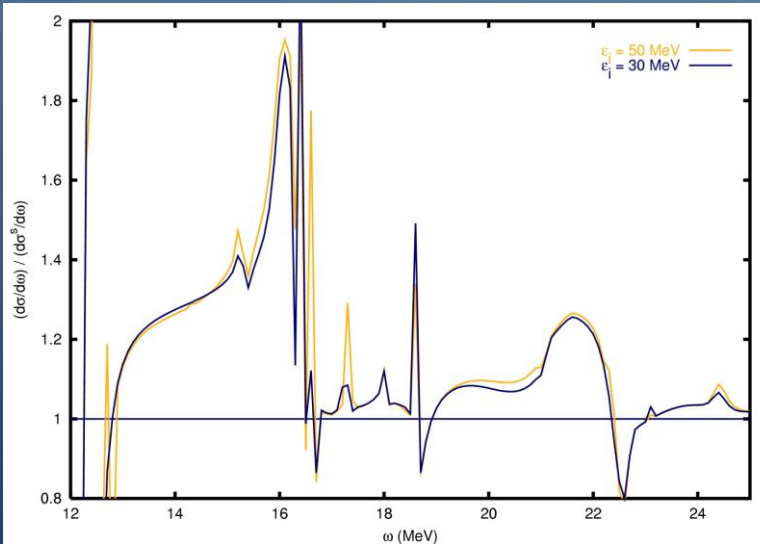
- vector current contributions are suppressed
- no radiative corrections



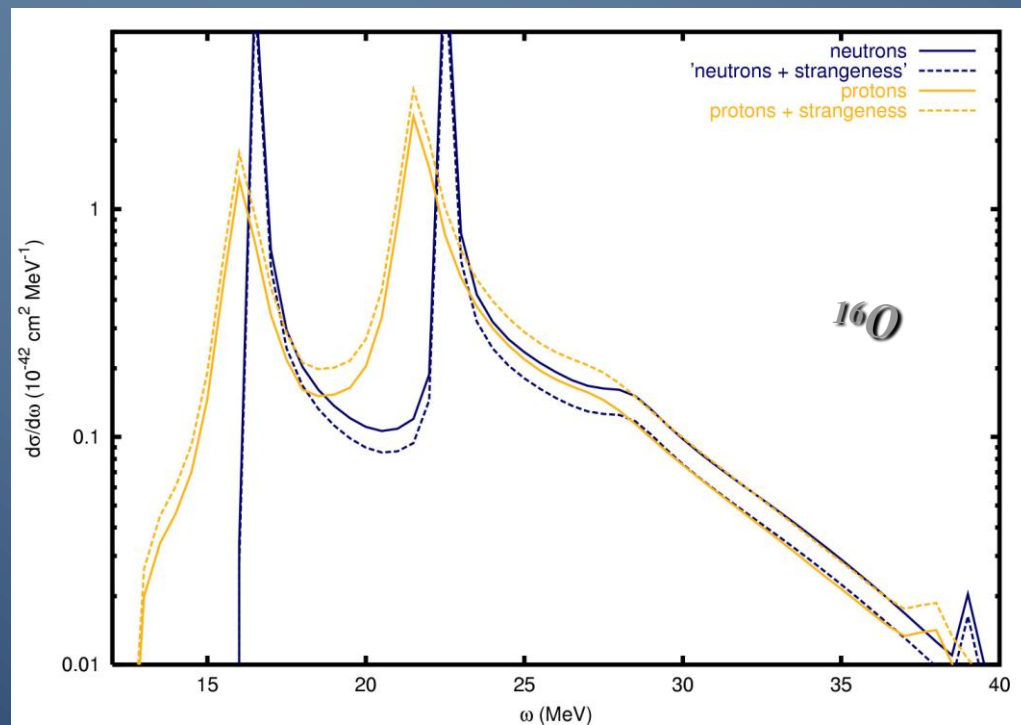
N.J., P. Vancraeyveld, P.
Lava, J. Ryckebusch,
PRC76, 055501 (2007).

Neutrino cross sections including strangeness

- Generally : net strangeness effect vanishes for isoscalar targets
- close to particle knockout threshold the influence becomes larger due to binding energy differences between protons and neutrons
- differential cross sections differ, energy of reaction products can be very different



proton/neutron cross sections

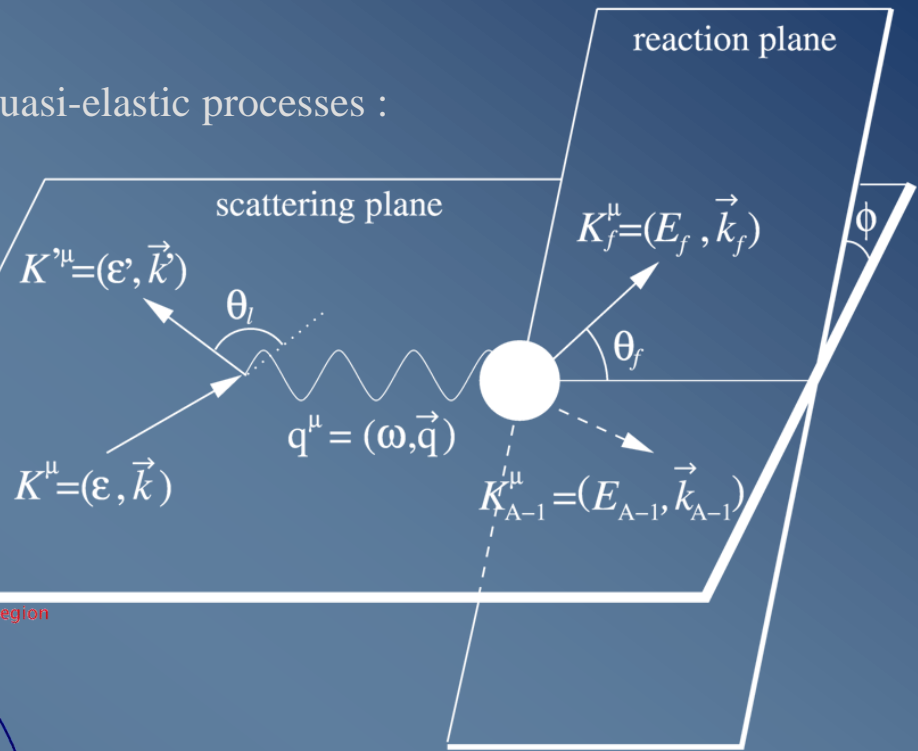


- differences up to 20%
- opposite effect for protons and neutrons

Oscillations and experiments at intermediate energies



Quasi-elastic processes :



Intermediate energies : 100 MeV - ... GeV

Energy distribution !

MiniBooNe Flux

Phys. Rev. D. 79, 072002 (2009)

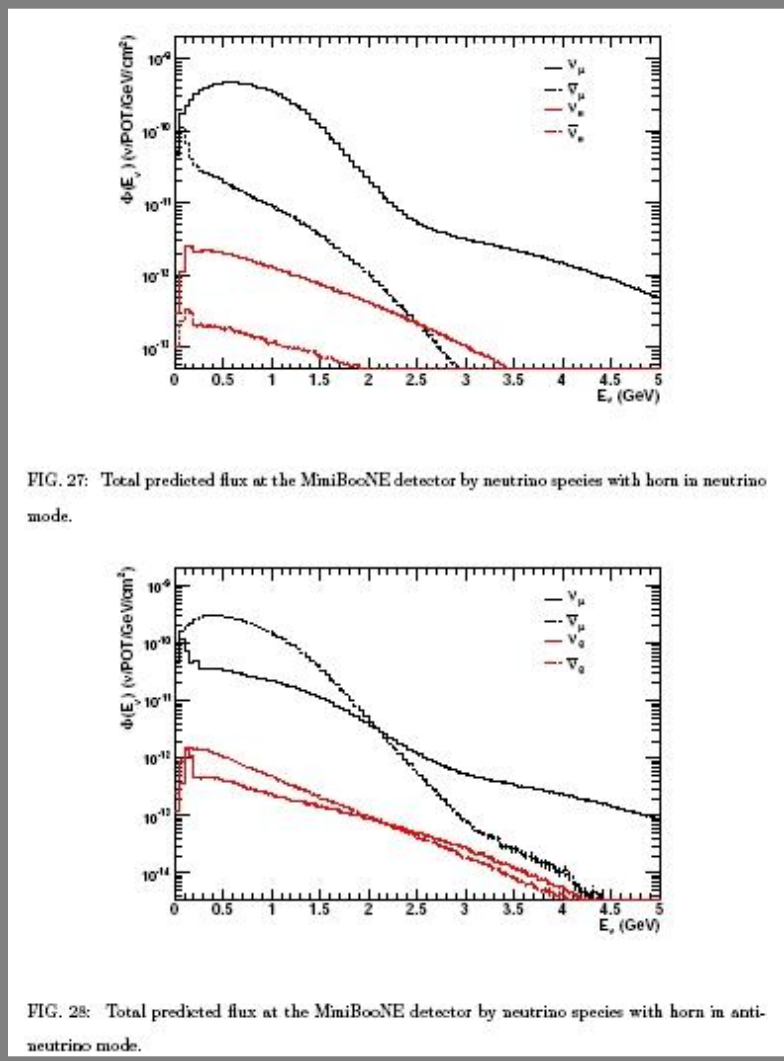


FIG. 27: Total predicted flux at the MiniBooNE detector by neutrino species with horn in neutrino mode.

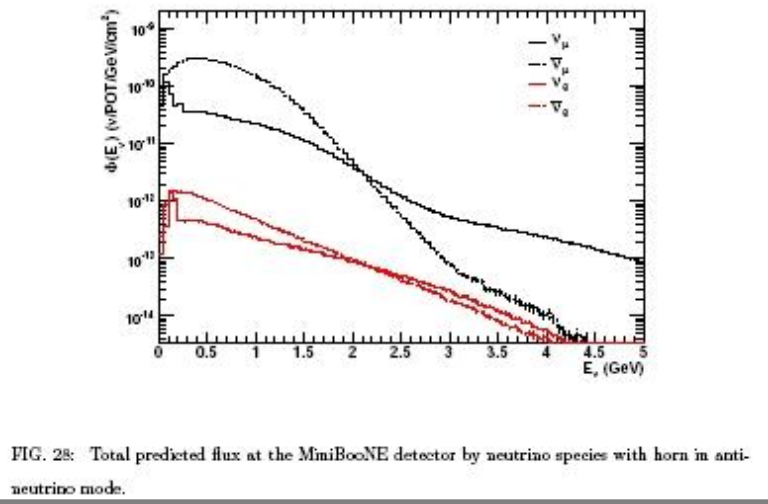
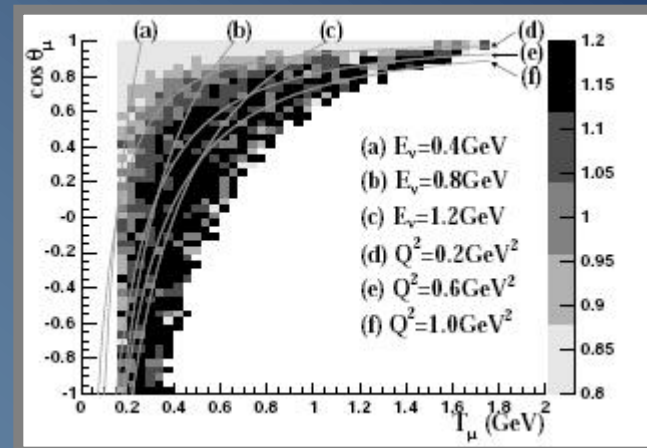
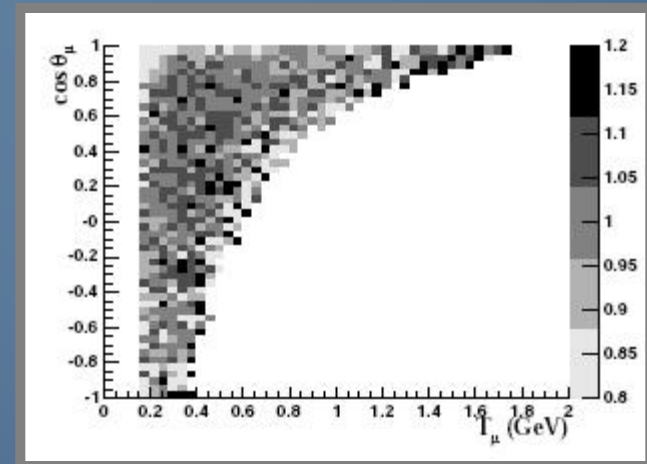


FIG. 28: Total predicted flux at the MiniBooNE detector by neutrino species with horn in anti-neutrino mode.



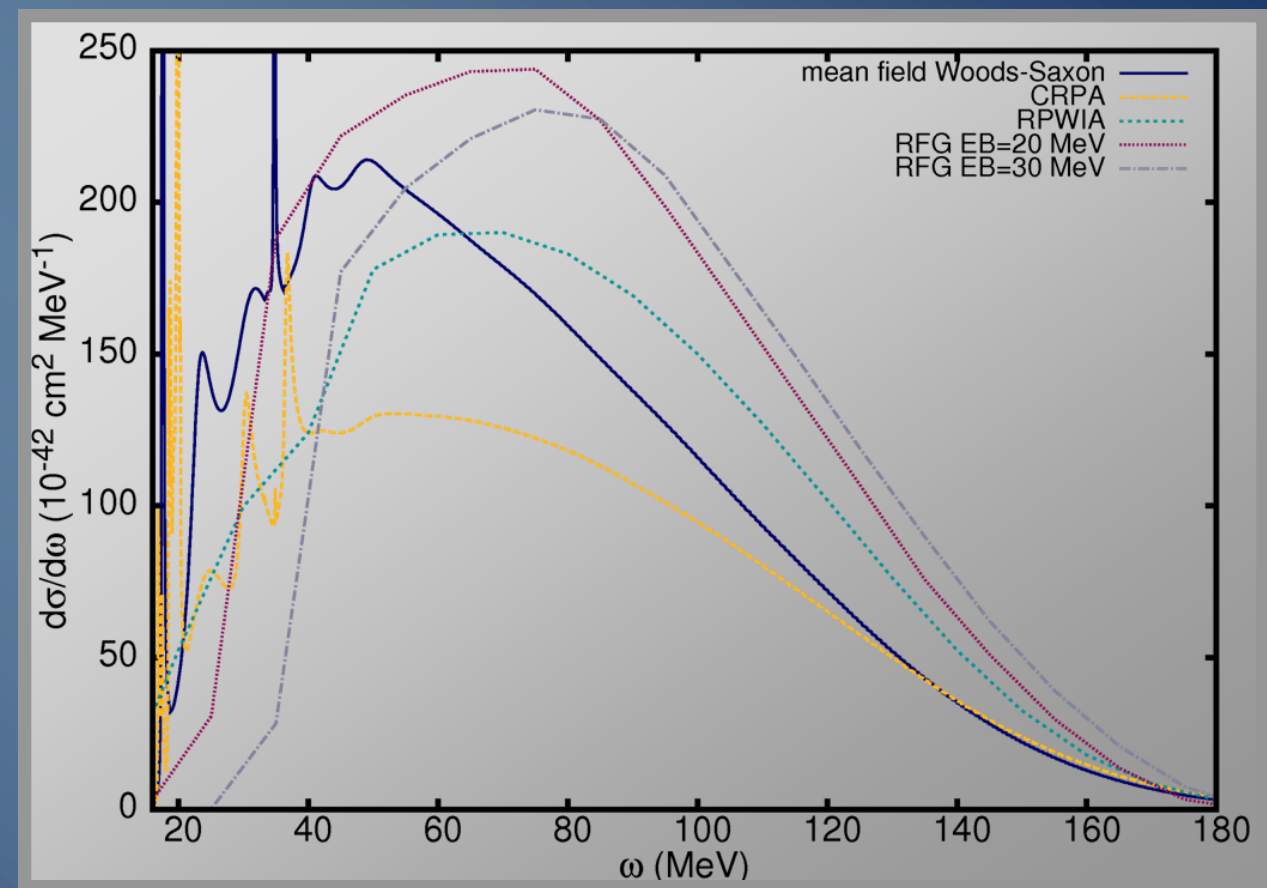
Modified Pauli-blocking ?



Phys. Rev. Lett. 100, 032301 (2008)

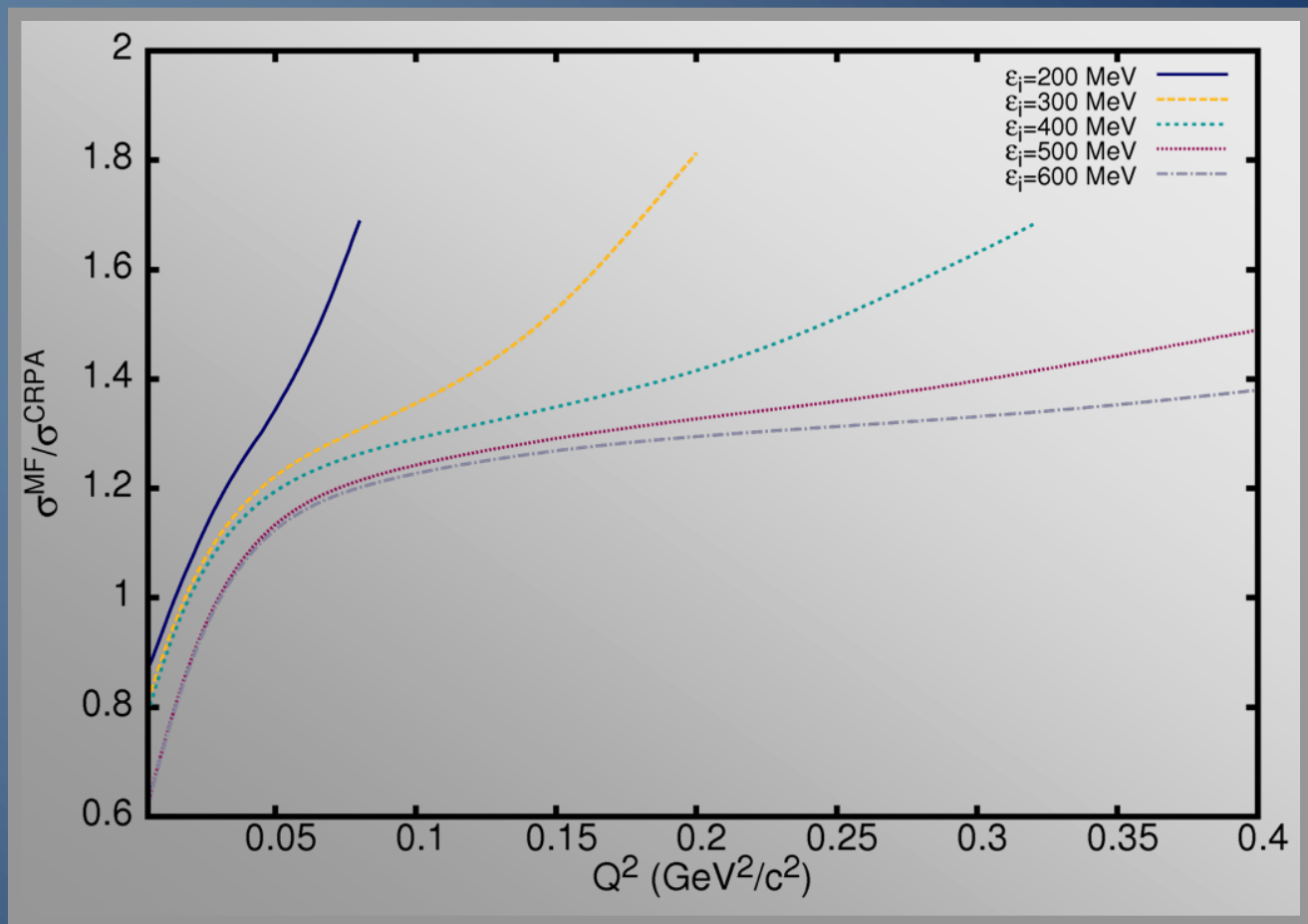
Cross sections at Low Q^2

Comparison between inclusive cross sections obtained within a relativistic Fermi gas calculation, a relativistic plane wave impulse approximation (RPWIA) approach, a mean-field calculation, and a calculation including CRPA correlations implemented using a Skyrme parametrization as residual interaction.



Cross sections at low Q^2

Q^2 dependence as
a function of
incoming energy



Supernova neutrino-nucleus interactions :

- Nucleosynthesis
- Terrestrial detection

Neutrino-nucleus reactions provide an interesting detection mechanism :

- relatively large cross sections
- thresholds in supernova-neutrino energy-region



The interpretation of the supernova signal can only be as good as the understanding of the neutrino-nucleus reaction that occurs in the detector

Low-energy neutrino-nucleus cross sections

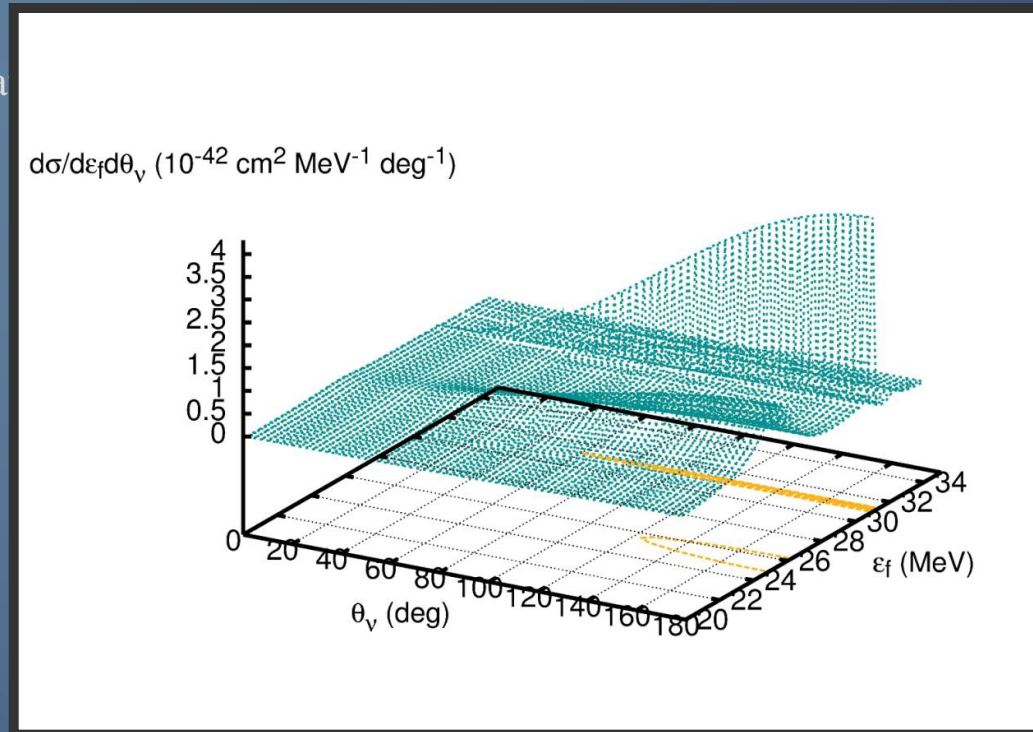
From the signal in the detector, one can obtain information about neutrinos and the supernova process :

- Arrival times

- black hole formation
- neutrino masses

- Directional information

- Scale



Low-energy neutrino-nucleus cross sections

From the signal in the detector, one can obtain information about neutrinos and the supernova process :

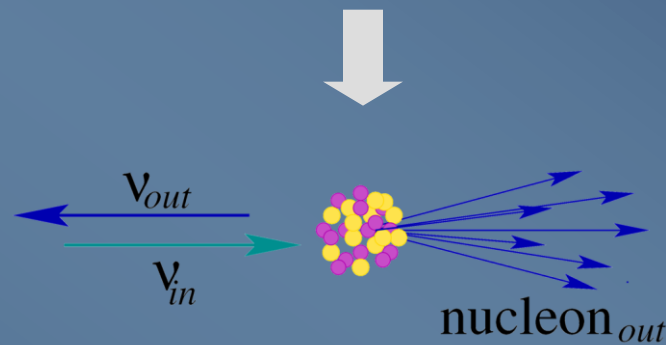
- **neutrino flavor**

- charge-exchange vs neutral-current reactions

- **neutrinos vs antineutrinos**

- charge of the outgoing lepton in charged-current reactions
- spin of the outgoing nucleon in neutral-current nucleon-knockout reactions

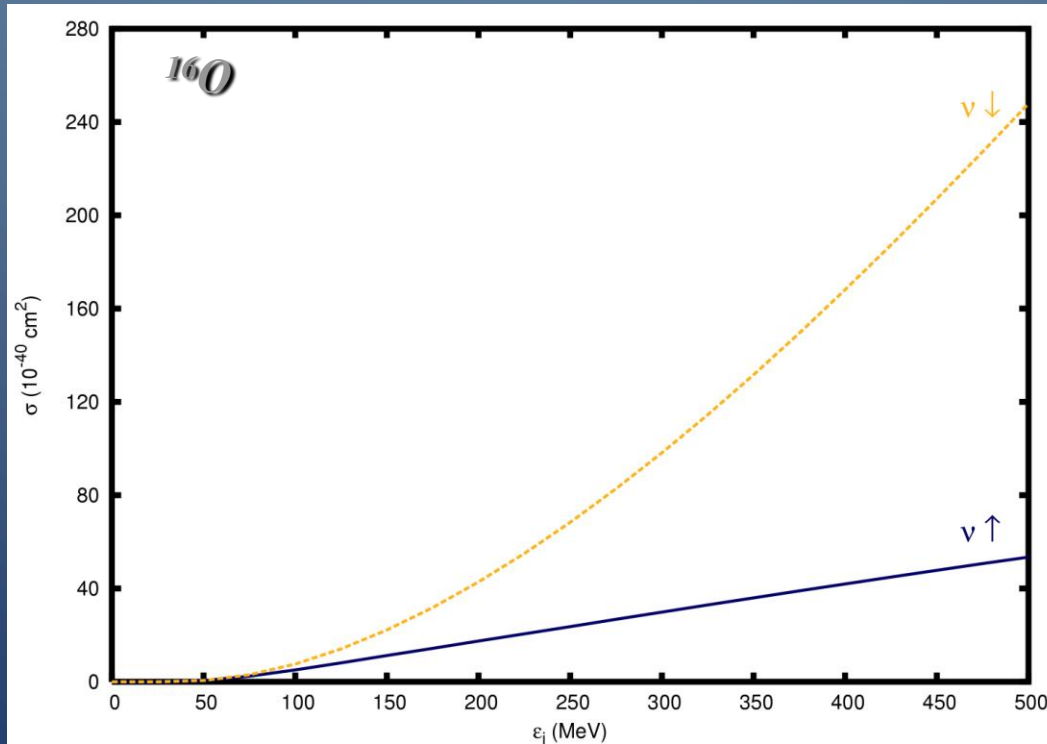
r : the ejectile's spin projection along the direction of the momentum transfer



for forward nucleon knockout, dominating in neutrino scattering, r tends to coincide with the longitudinal spin component of the ejectile

Helicity dependence of the cross section:

$$\begin{aligned}
 & l_- l_-^* h_+ h_+^* + l_+ l_+^* h_- h_-^* \\
 &= S(h_+ h_+^* + h_- h_-^*) + hA(h_+ h_+^* - h_- h_-^*) \\
 &= (S + hA)h_+ h_+^* + (S - hA)h_- h_-^*
 \end{aligned}$$



For neutrinos :

$S+hA = S-A$, is small

$S-hA = S+A$, is large



$h_- h_-^*$ dominates

For antineutrinos :

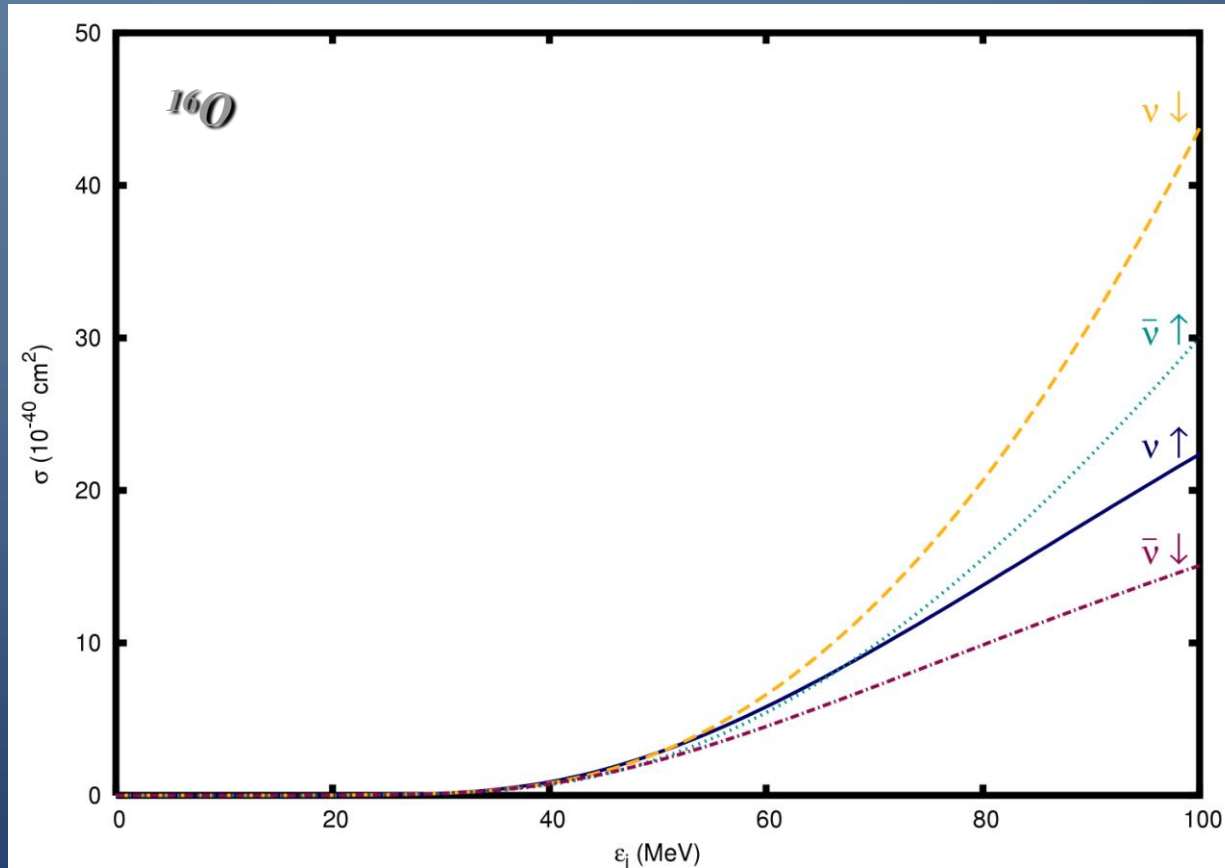
$S+hA = S+A$, is large

$S-hA = S-A$, is small



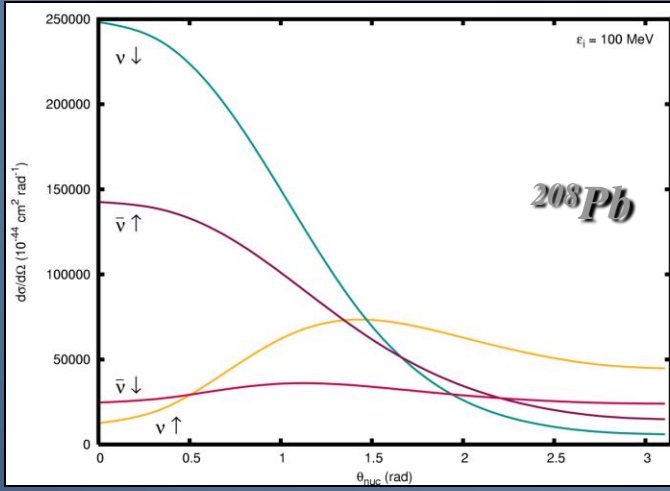
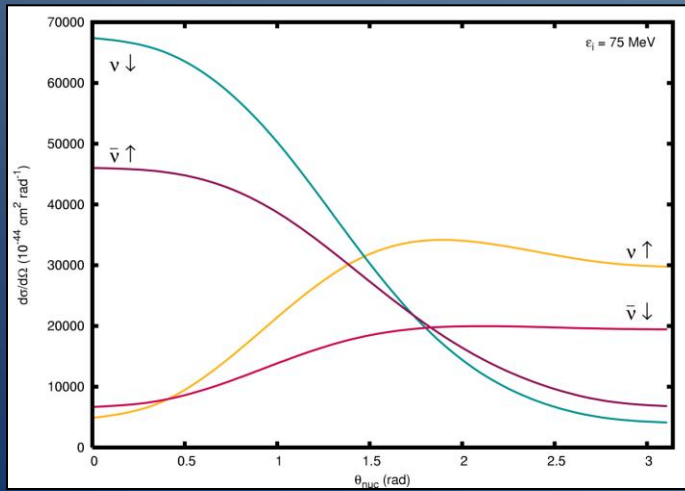
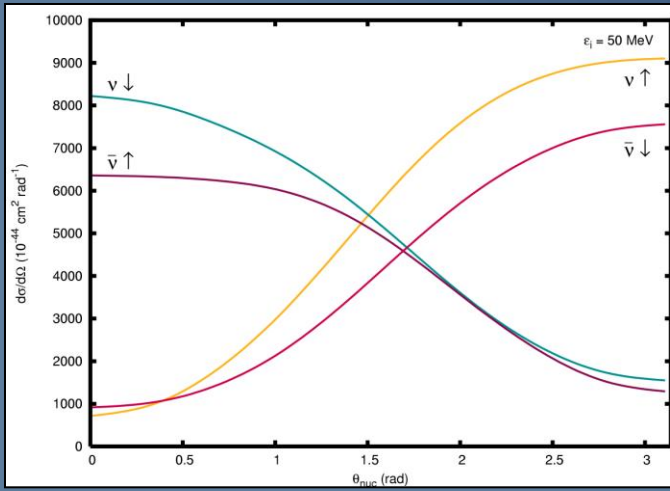
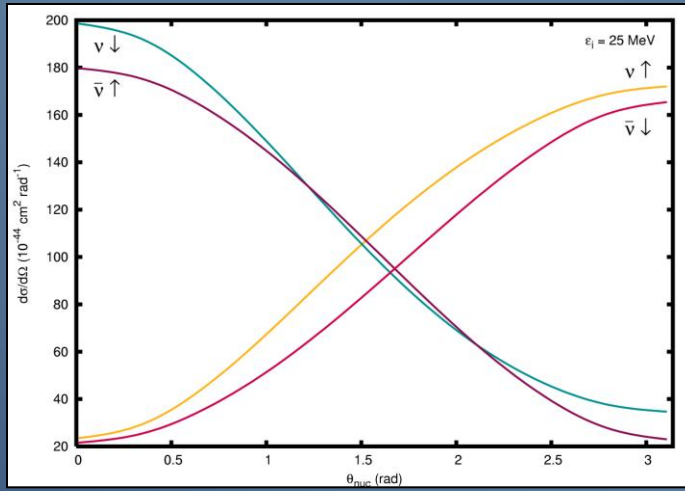
$h_+ h_+^*$ dominates

Adding antineutrinos to the picture :



- Neutrinos favor ‘spin down’ nucleon knockout
- Antineutrinos mainly induce ‘spin up’ knockout reactions
- Polarization differences increase with incoming neutrino energies

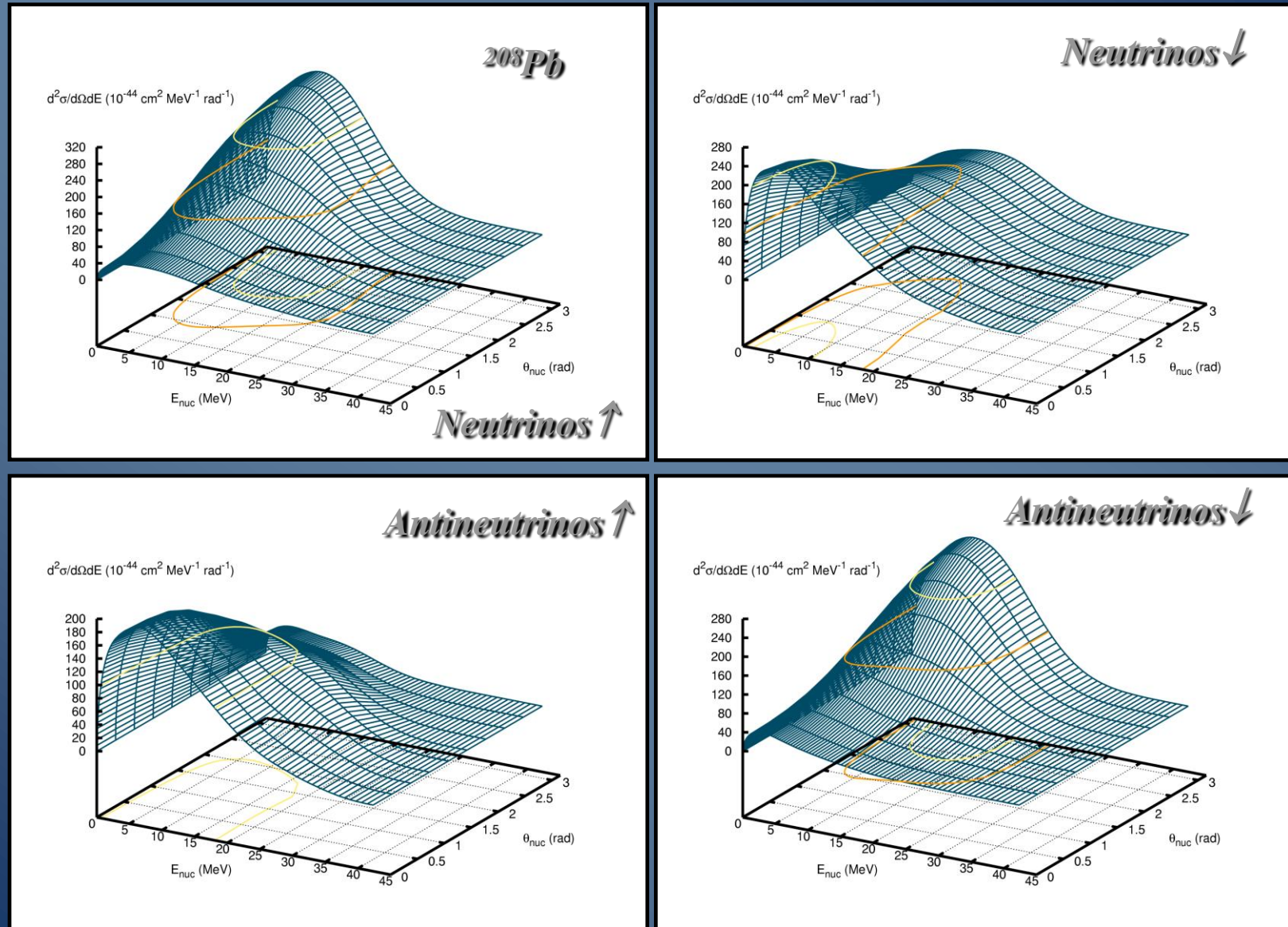
The asymmetry and the dissimilarities between neutrinos and antineutrinos are most clear considering the angular cross section :



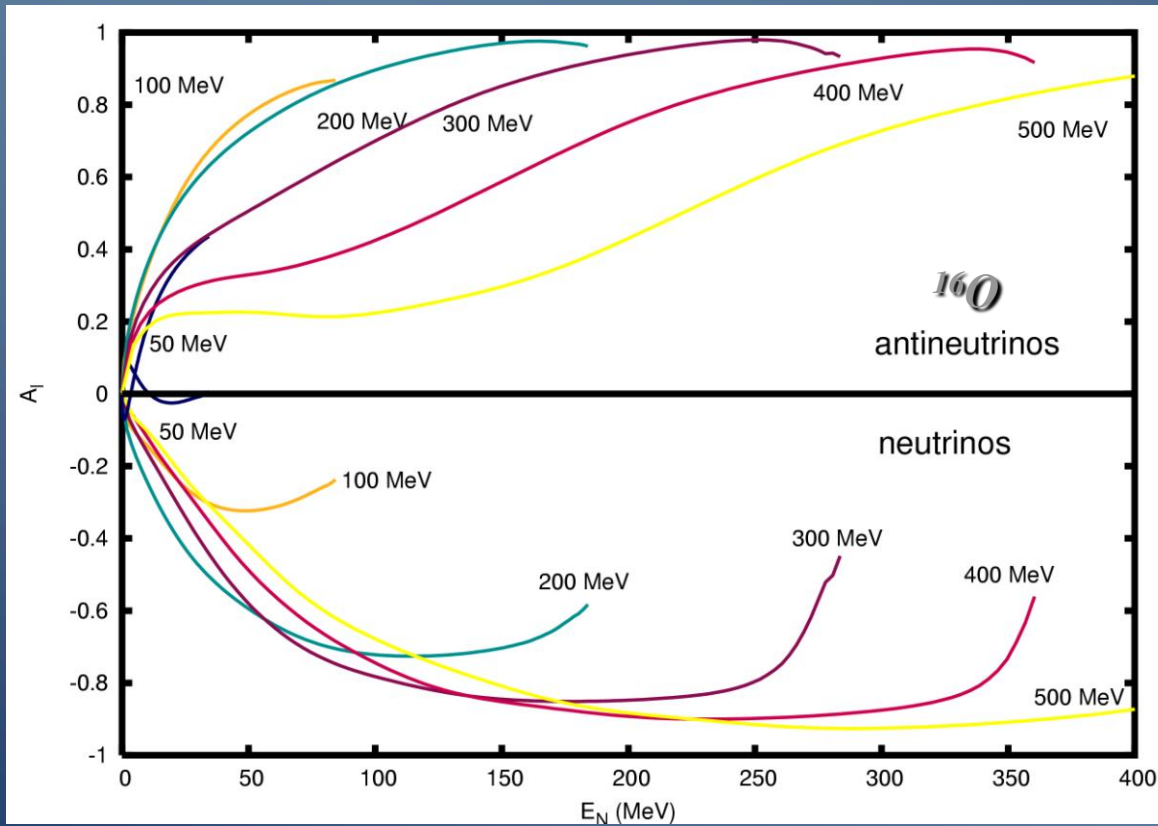
The asymmetry is most prominent for forward nucleon knockout, and remains large over a broad angular range.

For the suppressed backward scattering reactions, the asymmetry is completely reversed

Low-energy neutrino-nucleus cross sections



Longitudinal **polarization asymmetry** : $A_l = \frac{\sigma(s_N^l = \uparrow) - \sigma(s_N^l = \downarrow)}{\sigma(s_N^l = \uparrow) + \sigma(s_N^l = \downarrow)}$



- For antineutrinos, A_l is large and positive
- For neutrinos, A_l is large and negative

N. Jachowicz, K. Vantournhout, J. Ryckebusch, K. Heyde, PRL 93, 082501 (2004); N. Jachowicz, K. Vantournhout, J. Ryckebusch, K. Heyde, PRC71, 034604 (2005).

Low-energy neutrino-nucleus cross sections

From the signal in the detector, one can obtain information about neutrinos and the supernova process :

- **neutrino flavor**

- charge-exchange vs neutral-current reactions

- **neutrinos vs antineutrinos**

- charge of the outgoing lepton in charged-current reactions
- spin of the outgoing nucleon in neutral-current nucleon-knockout reactions

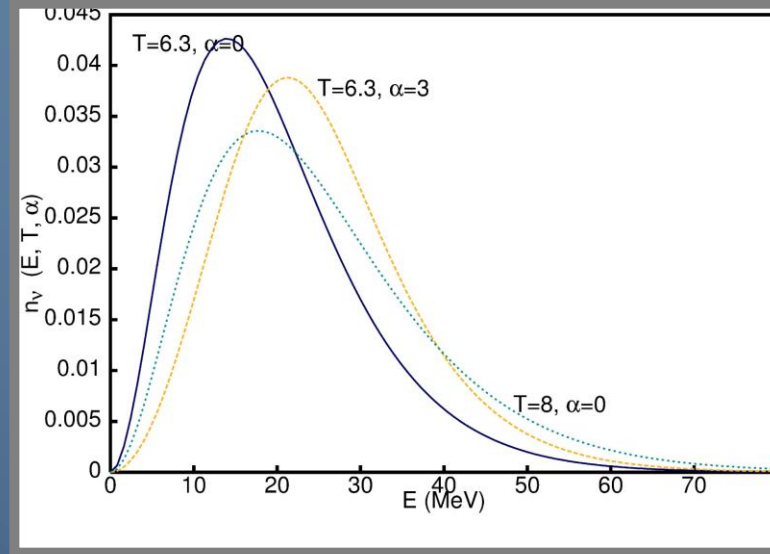
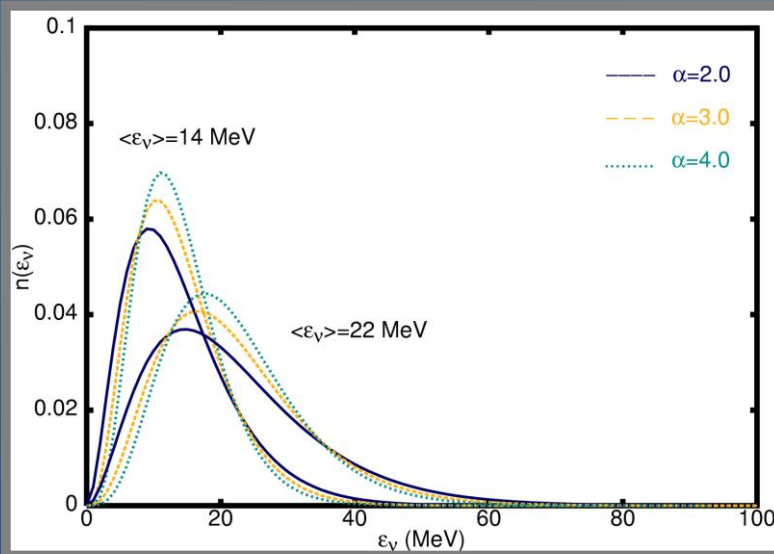
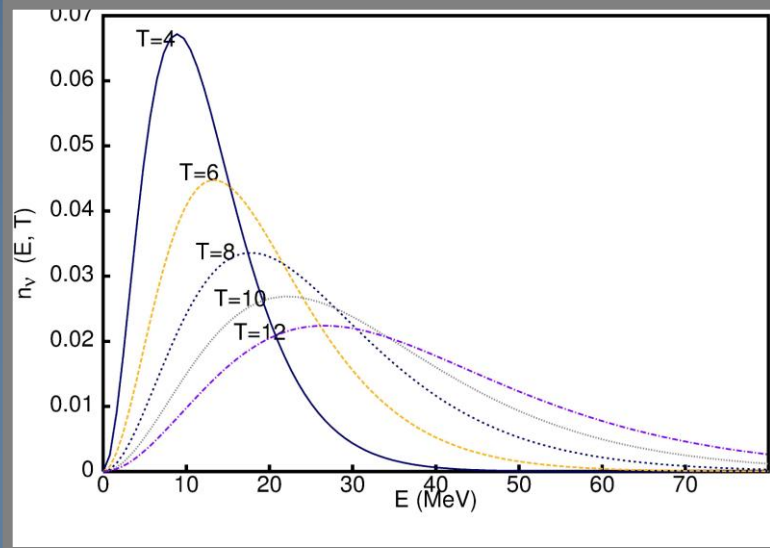
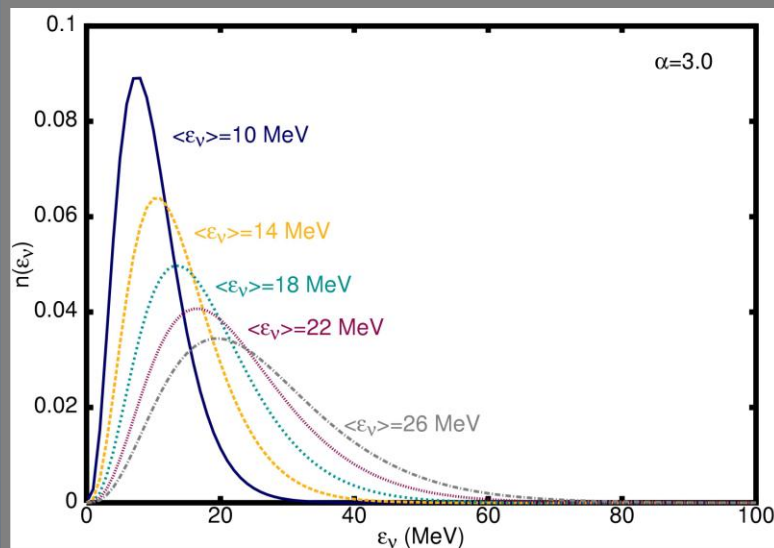
- **energy information**

- threshold differences between different nuclei
- 1 nucleon vs 2 nucleon knockout

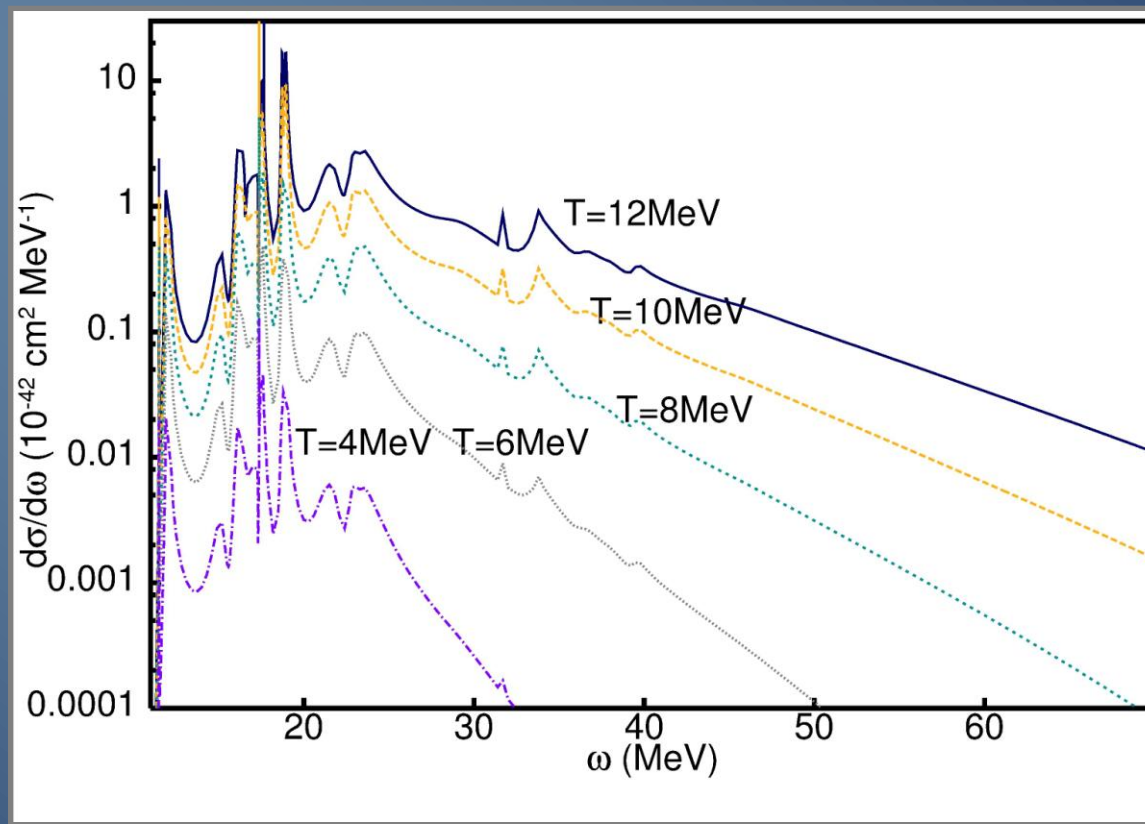
Low-energy neutrino-nucleus cross sections

Supernova neutrino spectra :

$$n_{SN[\langle \varepsilon \rangle, \alpha]}(\varepsilon) = \left(\frac{\varepsilon}{\langle \varepsilon \rangle} \right)^\alpha e^{-(\alpha+1)\frac{\varepsilon}{\langle \varepsilon \rangle}}$$



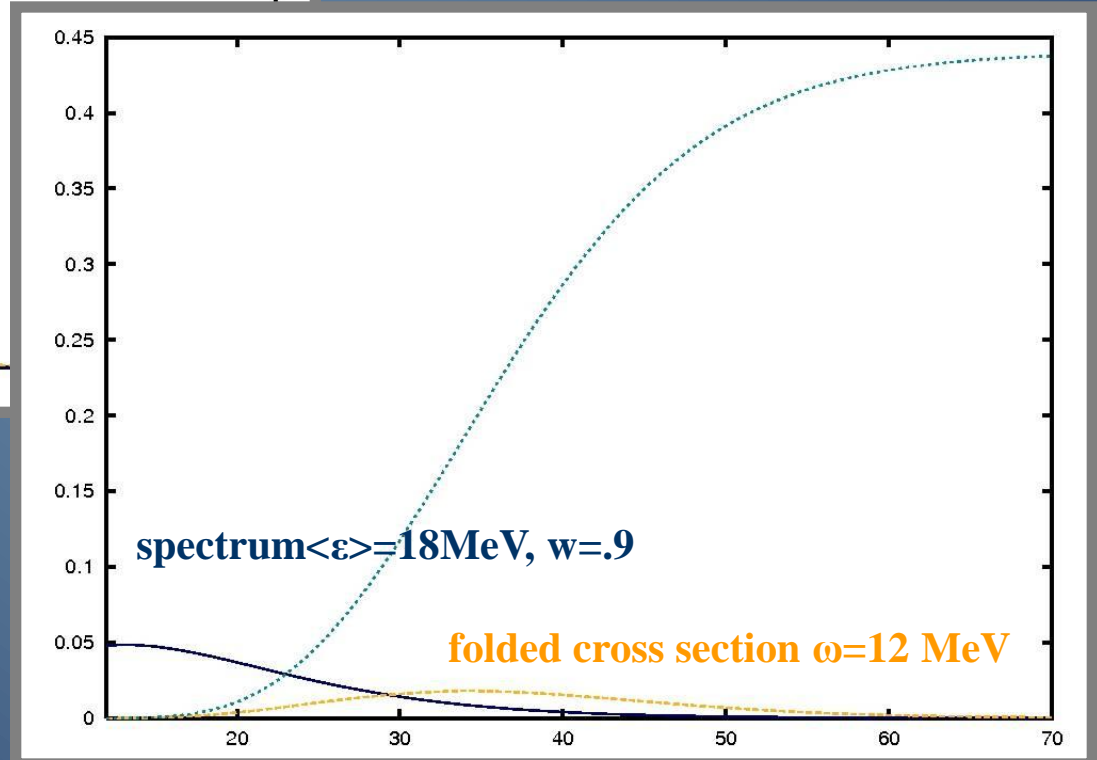
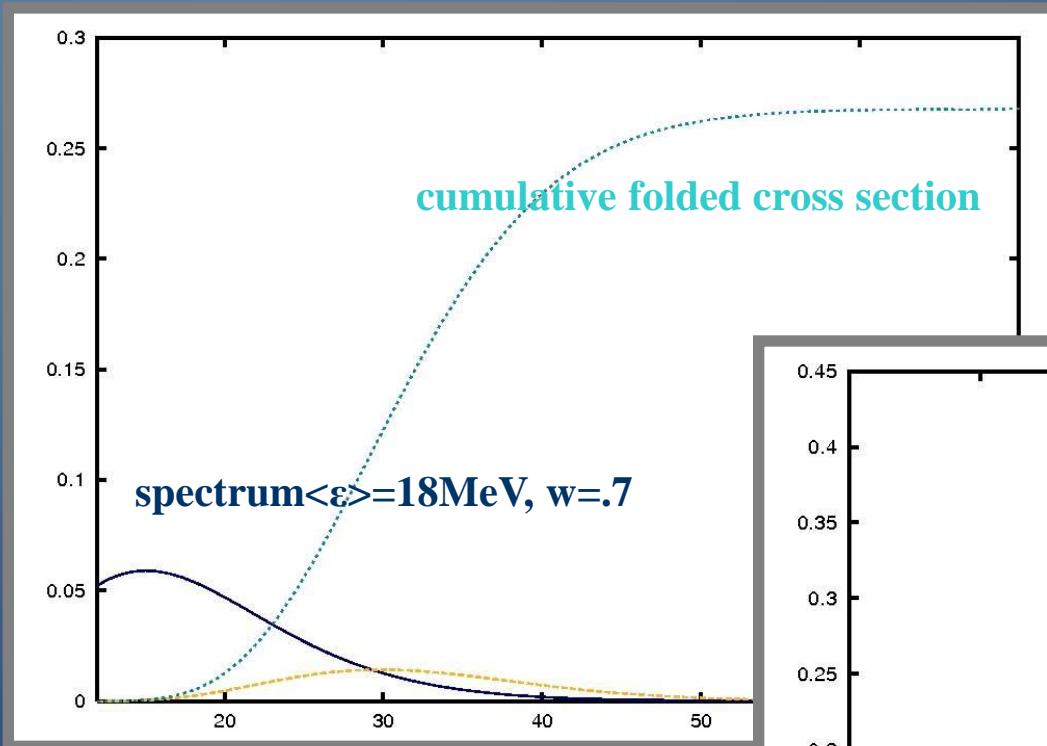
Low-energy neutrino-nucleus cross sections



Low-energy neutrino-nucleus cross sections

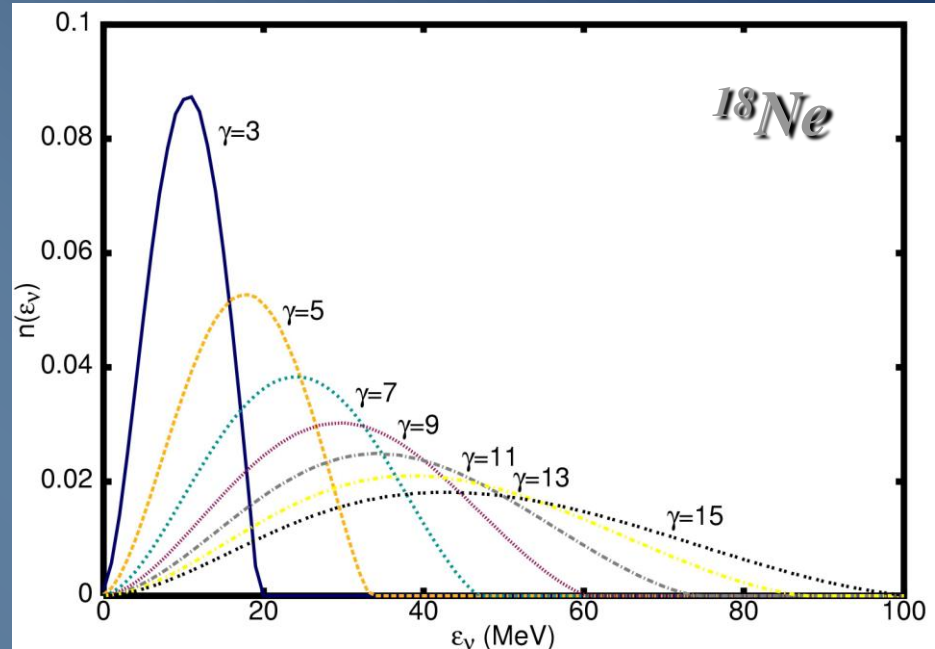
Supernova neutrino spectra :

$$n_{SN[\langle \epsilon \rangle, \alpha]}(\varepsilon) = \left(\frac{\varepsilon}{\langle \varepsilon \rangle} \right)^\alpha e^{-(\alpha+1)\frac{\varepsilon}{\langle \varepsilon \rangle}}$$



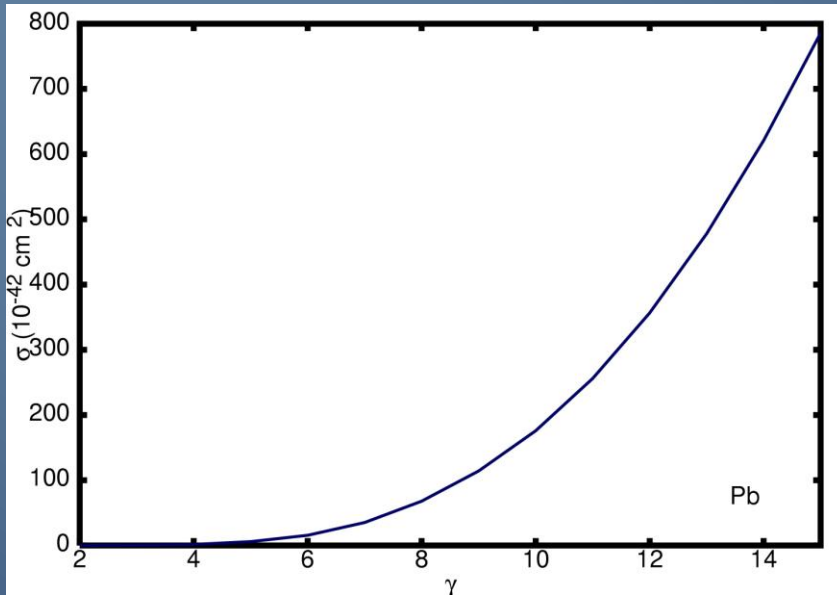
Beta-beam neutrino spectra :

- β -decay of a primary beam of boosted ions generates intense neutrino beams,
- with average energy and precise shape of the spectrum determined by the boost factor γ of the primary beam



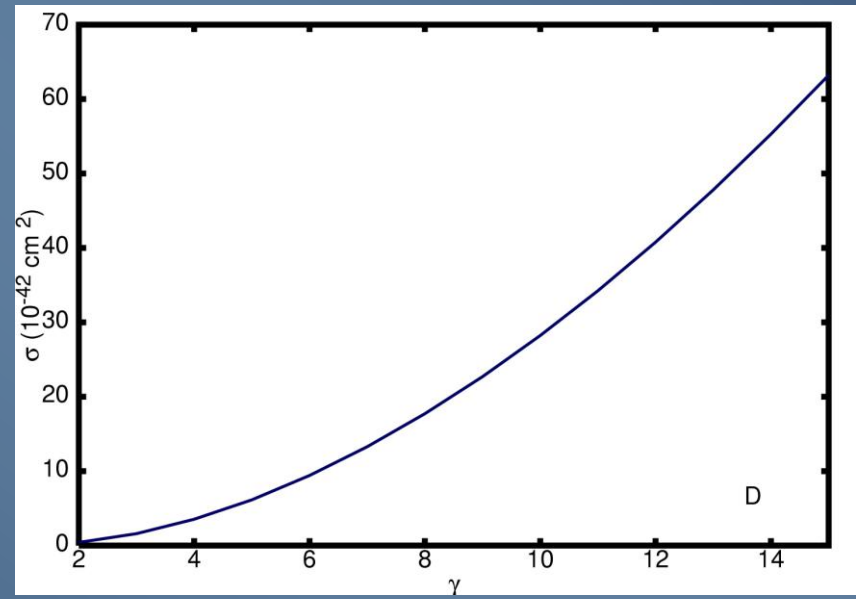
- First proposed to produce high energy neutrinos in oscillation experiments
(P.Zucchelli, Phys.Lett.B 532, 166 (2002)).
- At lower gamma factor, the neutrino energy becomes very suitable for neutrino-nucleus scattering investigations
(C. Volpe, J.Phys. G30, 1 (2004)).

Low-energy neutrino-nucleus cross sections



Cross section as a function of the boost factor γ of the beam

$$\sigma_\gamma^{fold} = \int_0^\infty d\varepsilon_i \sigma(\varepsilon_i) n^\gamma(\varepsilon_i)$$



Procedure :

- linear combinations of normalized beta-beam spectra :

$$n_{N\gamma}(\varepsilon_i) = \sum_{i=1}^N a_i n_{\gamma_i}(\varepsilon_i)$$

$$\int d\varepsilon_i n_{\gamma_i}(\varepsilon_i) = 1 \quad \forall i$$

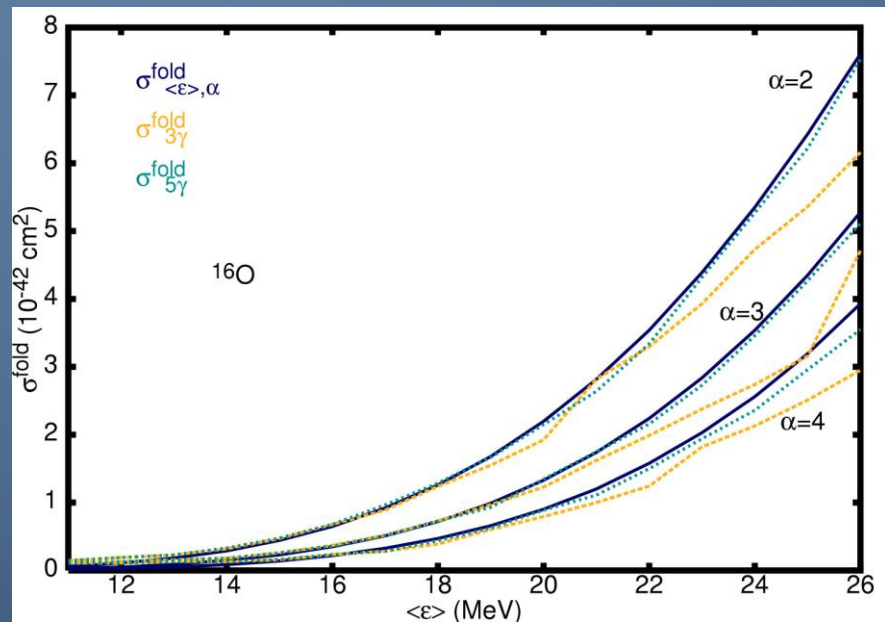
$$\int d\varepsilon_i n_{N\gamma}(\varepsilon_i) = 1$$

- fitting the constructed energy distribution to the supernova-neutrino spectrum by minimizing the expression,

$$\int_{\varepsilon_i} d\varepsilon_i |n_{N\gamma}(\varepsilon_i) - n_{SN}(\varepsilon_i)|$$

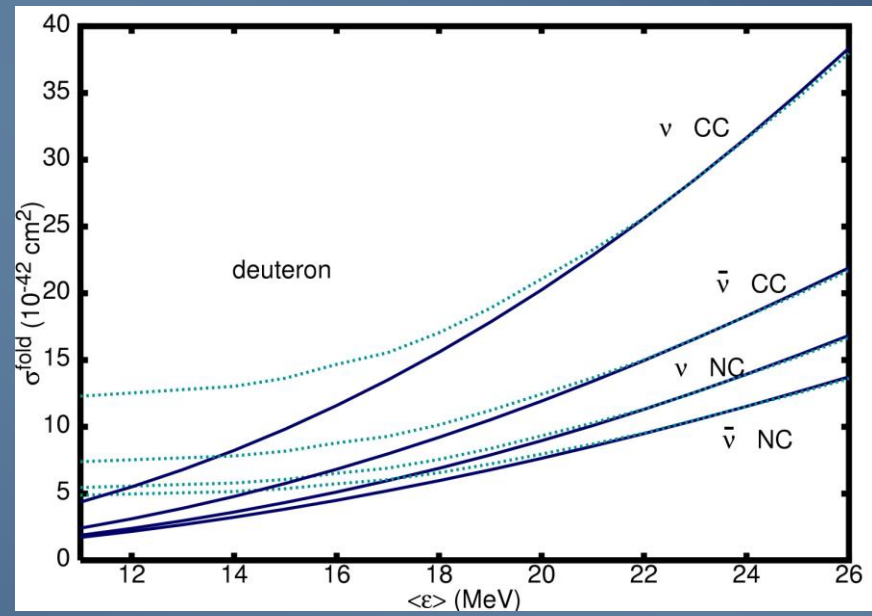
$$n_{SN[\langle \varepsilon \rangle, \alpha]}(\varepsilon) = \left(\frac{\varepsilon}{\langle \varepsilon \rangle} \right)^\alpha e^{-(\alpha+1)\frac{\varepsilon}{\langle \varepsilon \rangle}}$$

varying the expansion parameters a_i and the boost factors γ_i



- ^{16}O : CRPA calculation
- deuteron : S. Nakamura, T. Sato, S. Ando et al.,
Nucl. Phys. A 707 (2002)

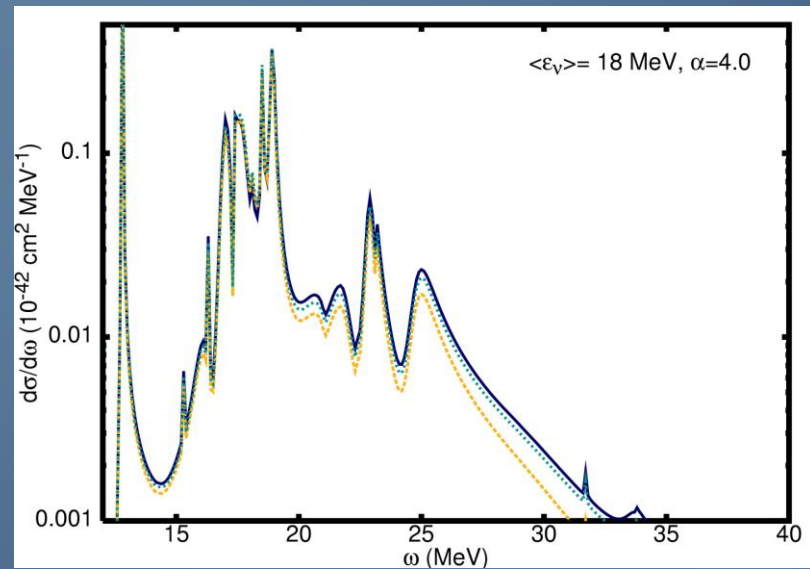
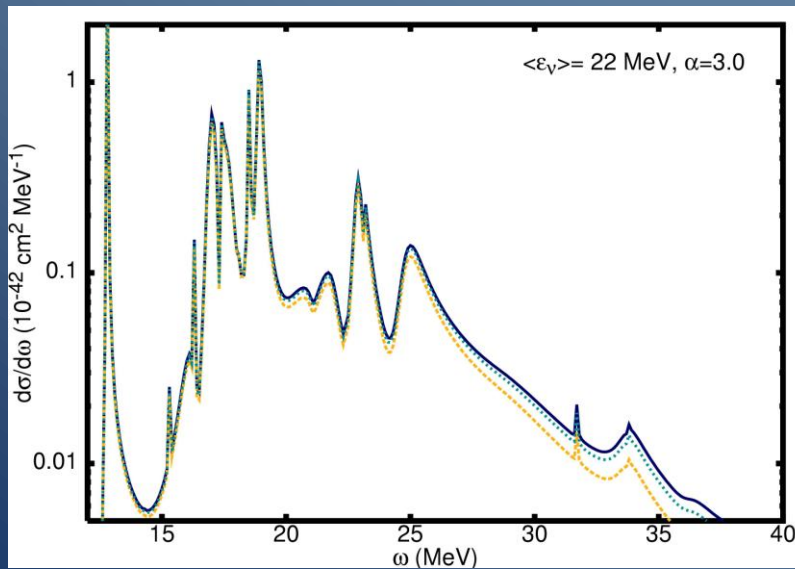
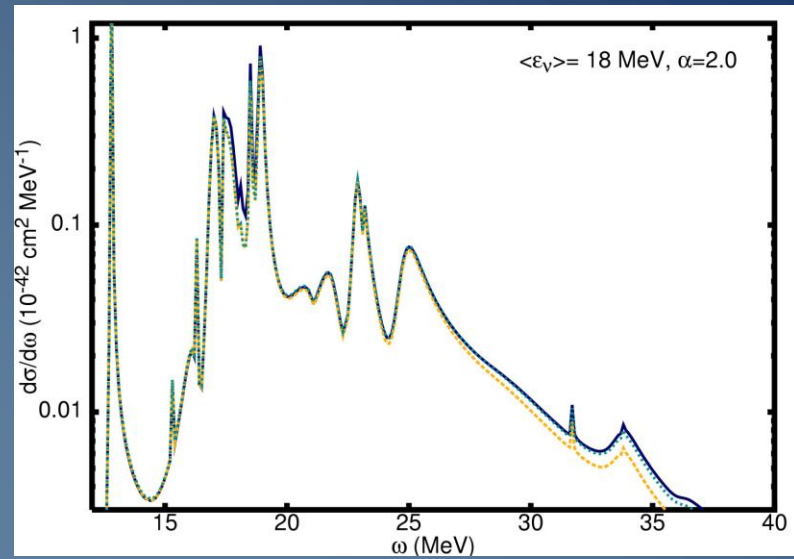
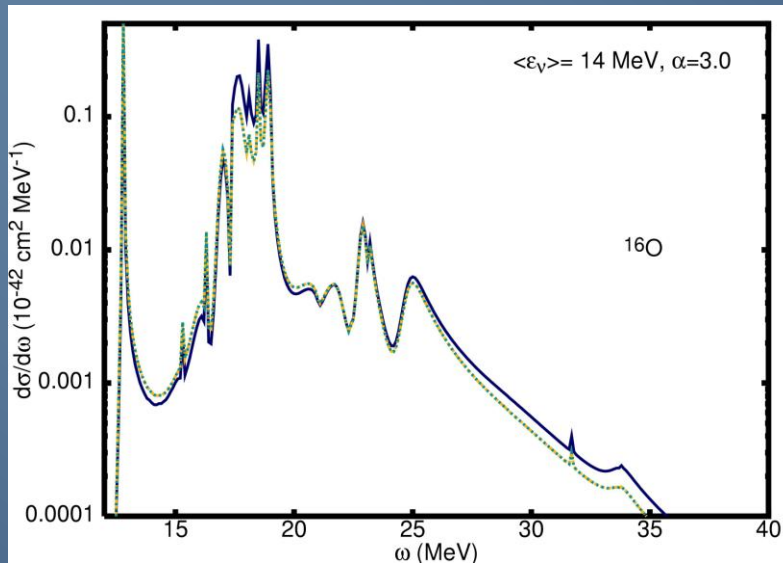
Total folded cross sections :



Low-energy neutrino-nucleus cross sections

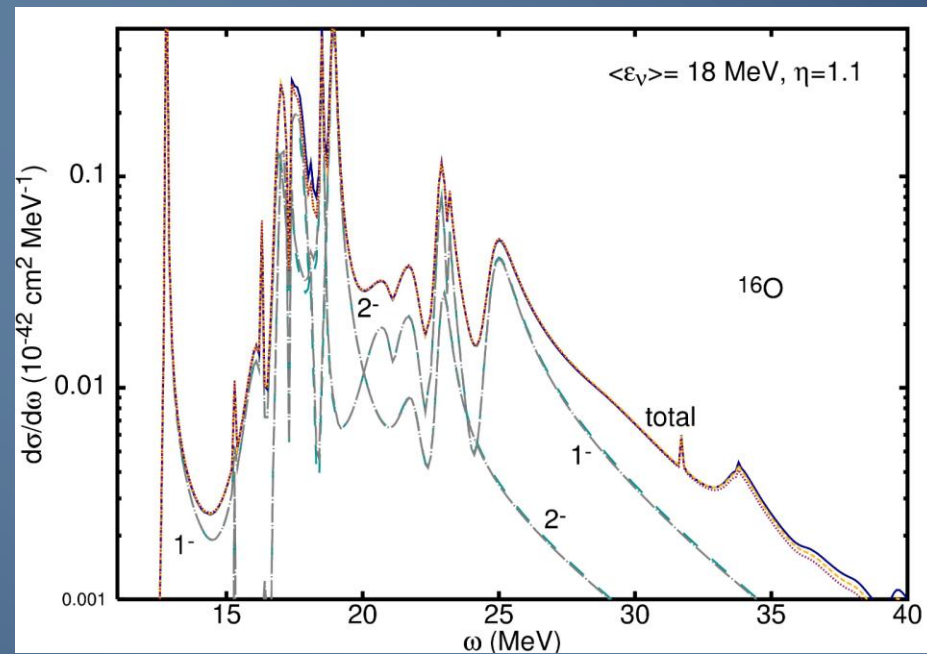
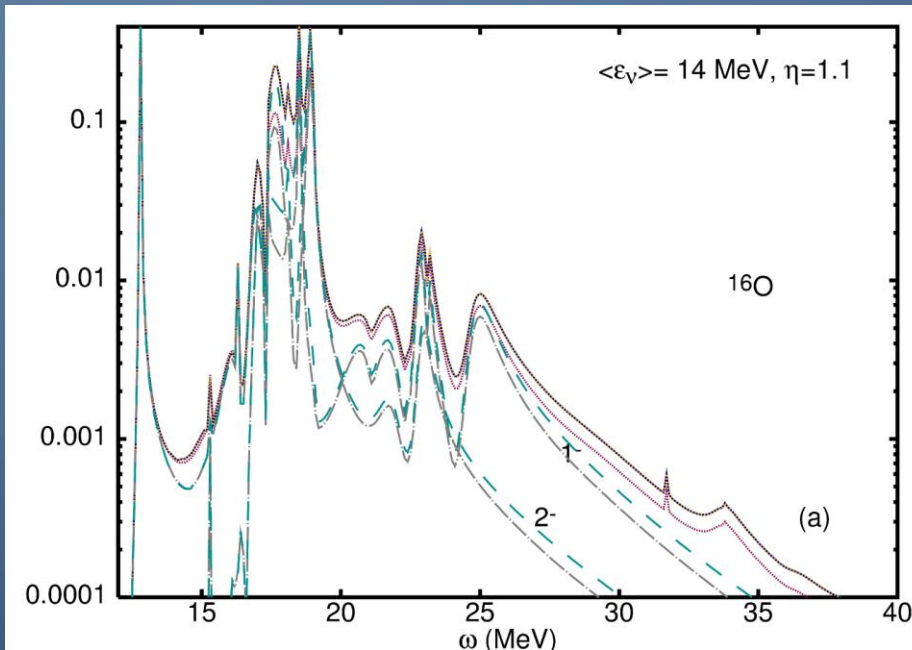
^{16}O

... differential folded cross sections



Low-energy neutrino-nucleus cross sections

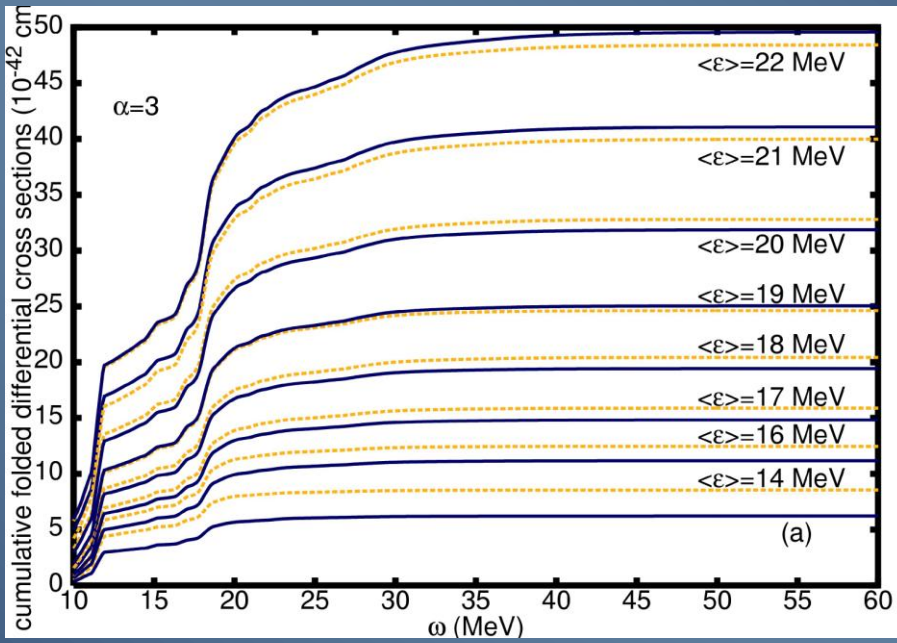
... differential folded cross sections –multipole contributions



 This very satisfying agreement suggests that it is possible to reconstruct supernova-neutrino signal using the results of the beta-beam measurement without going through the intermediate step of using a nuclear structure calculation

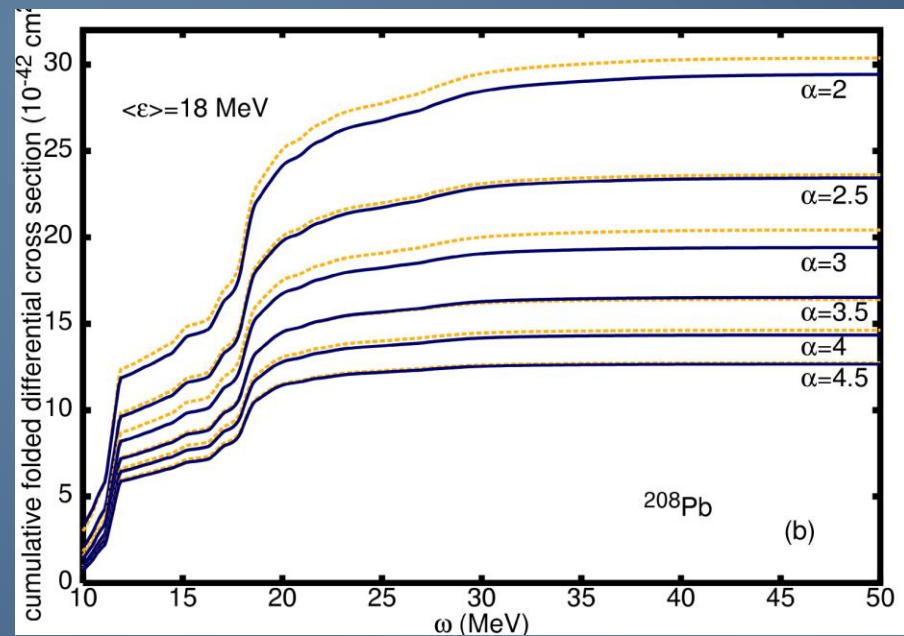
- For each set of beta-beam data at a given γ , there will be a measured response in the detector
- Taking appropriate linear combinations of the measured response provides a very accurate picture of the response of the detector to an incoming supernova-neutrino spectrum

Low-energy neutrino-nucleus cross sections

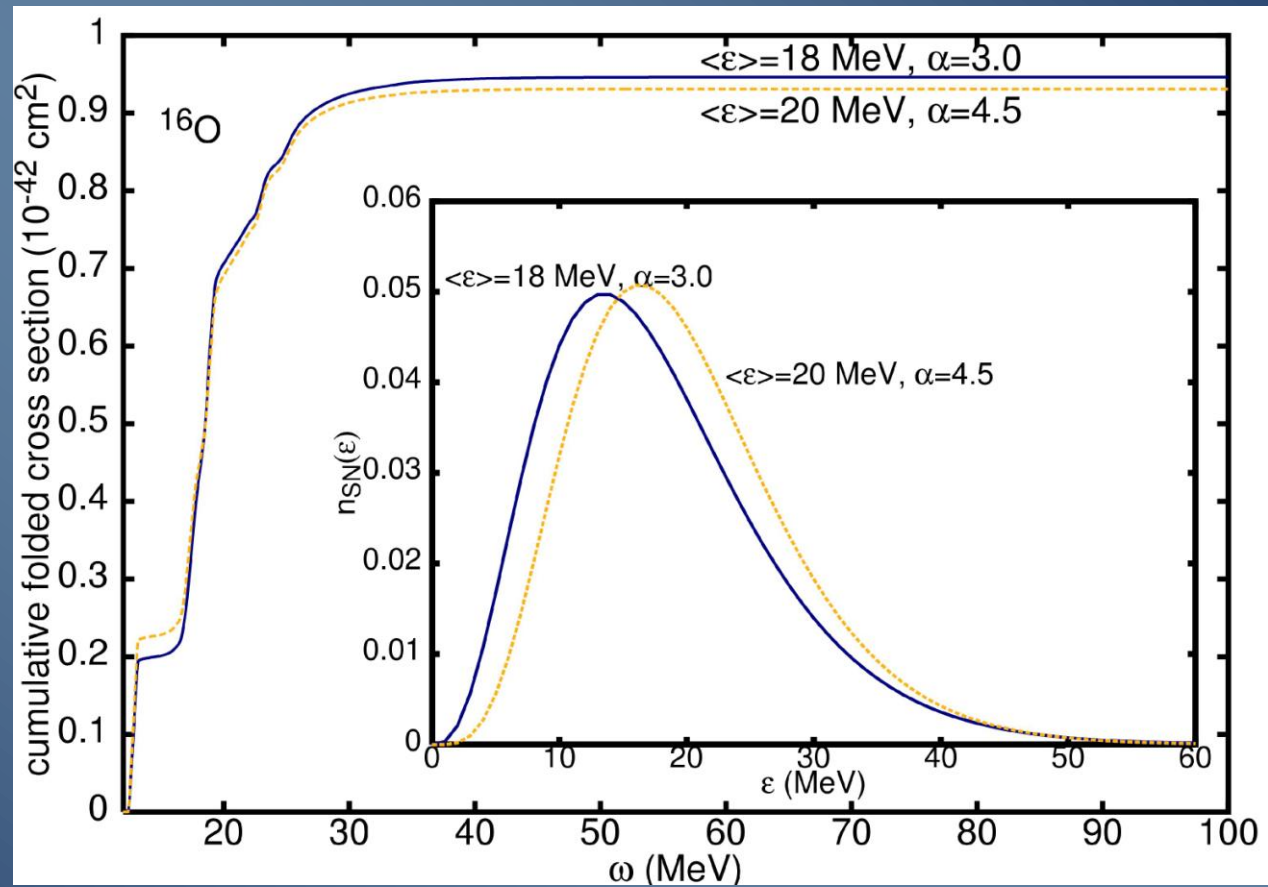


Width ‘resolution’

Energy ‘resolution’



Reconstructing the supernova neutrino spectrum ?



Inversion of the method : reconstructing the supernova neutrino energy spectrum

Supernova neutrino signal in a terrestrial detector

$$\sigma_{signal}^{fold}(\omega) = \int d\varepsilon_\nu \sigma(\varepsilon_\nu, \omega) n_{SN}(\varepsilon_\nu).$$

Fit with linear combination of beta beam responses :

$$\sigma_{fit}^{fold}(\omega) = \sum_{i=1}^N a^{\gamma_i} \int d\varepsilon_\nu \sigma(\varepsilon_\nu, \omega) n^{\gamma_i}(\varepsilon_\nu)$$

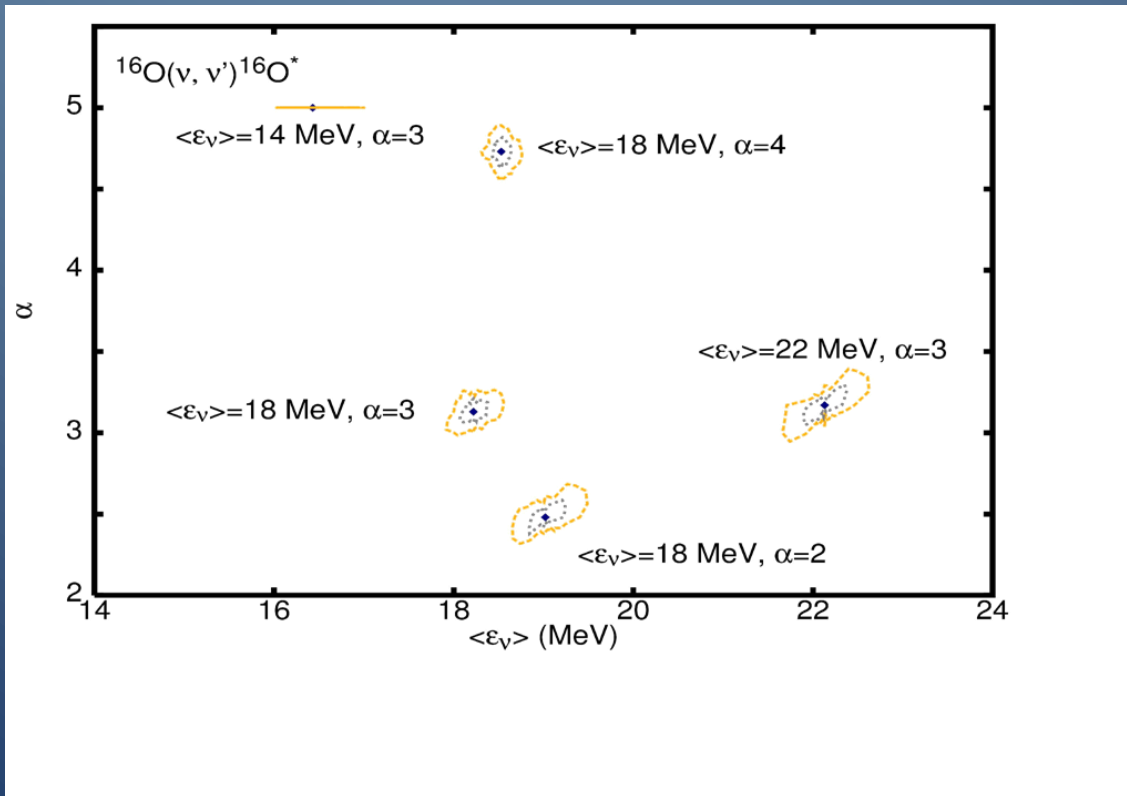


$$a^{\gamma_i}, \gamma_i$$



$$n_{SN}$$

Inversion of the method – reconstruction in terms of average energy and width of the spectrum



curves : 90% confidence levels for spectra with
5 and 10 % uncertainty on the expansion parameters

N.J., G. McLaughlin,
PRL96, 172301 (2006) ;
N.J., G. McLaughlin, C.
Volpe, PRC77, 055501
(2008)

